Energetics underlying hemin extraction from human hemoglobin by *Staphylococcus aureus*

Received for publication, November 8, 2017, and in revised form, February 23, 2018 Published, Papers in Press, March 14, 2018, DOI 10.1074/jbc.RA117.000803

Megan Sjodt[‡§1], Ramsay Macdonald[‡§2], Joanna D. Marshall[‡], Joseph Clayton[¶], John S. Olson[‖3], Martin Phillips[‡], David A. Gell[**], Jeff Wereszczynski[¶], and Robert T. Clubb[‡§‡‡4]

From the [‡]Department of Chemistry and Biochemistry, [§]UCLA-DOE Institute of Genomics and Proteomics, and [‡‡]Molecular Biology Institute, UCLA, Los Angeles, California 90095, the [¶]Department of Physics and Center for Molecular Study of Condensed Soft Matter, Illinois Institute of Technology, Chicago, Illinois 60616, the [‖]Department of BioSciences, Rice University, Houston, Texas 77251, and the [**]School of Medicine, University of Tasmania, Hobart, Tasmania 7000, Australia

Edited by Joseph M. Jez

Staphylococcus aureus **is a leading cause of life-threatening infections in the United States. It actively acquires the essential nutrient iron from human hemoglobin (Hb) using the iron-regulated surface-determinant (Isd) system. This process is initiated when the closely related bacterial IsdB and IsdH receptors bind to Hb and extract its hemin through a conserved tri-domain unit that contains two NEAr iron Transporter (NEAT) domains that are connected by a helical linker domain. Previously, we demonstrated that the tri-domain unit within IsdH ($IsdH^{N2N3}$) triggers hemin release by distorting Hb's F-helix. Here, we report that $IsdH^{N2N3}$ promotes hemin release from both the α- and β-subunits. Using a receptor mutant that only binds to the α-subunit of Hb and a stopped-flow transfer assay, we determined the energetics and micro-rate constants of hemin extraction from tetrameric Hb. We found that at 37 °C, the receptor accelerates hemin release from Hb up to 13,400-fold, with an activation enthalpy of 19.5 ± 1.1 kcal/mol. We propose that hemin removal requires the rate-limiting hydrolytic cleavage of the axial HisF8 Nϵ–Fe^{3+} bond, which, based on molecular dynamics simulations, may be facilitated by receptor-induced bond hydration. Isothermal titration calorimetry experiments revealed that two distinct $IsdH^{N2N3}$·Hb protein·protein interfaces promote hemin release. A high-affinity receptor·Hb(A-helix) interface contributed ~95% of the total binding standard free energy, enabling much weaker receptor interactions with Hb's F-helix that distort its hemin pocket and cause unfavorable changes in the binding enthalpy. We present a model indicating that receptor-introduced structural distortions and increased solvation underlie the IsdH-mediated hemin extraction mechanism.**

This work was supported in part by National Science Foundation Grant MCB-1716948 (to R. T. C. and J. W.) and National Institutes of Health Grants AI52217 (to R. T. C.), R35GM119647 (to J. W.), F31GM101931 (to M. S.), and P01-HL110900 (to J. S. O.). The authors declare that they have no conflicts of interest with the contents of this article. The content is solely the responsibility of the authors and does not necessarily represent the official views of the National Institutes of Health.

[1] Present address: Harvard Medical School Dept. of Biological Chemistry and Molecular Pharmacology Boston, MA 02115.

[2] Supported by National Institutes of Health Cellular and Molecular Biology Training (Ruth L. Kirschstein) NRSA Research Service Award GM007185.

[3] Supported by Robert A. Welch Foundation Grant C-0612.

[4] To whom correspondence should be addressed: Dept. of Chemistry and Biochemistry, UCLA, 602 Boyer Hall, Los Angeles, CA 90095. Tel.: 310-206-2334; Fax: 310-206-4749; E-mail: rclubb@mbi.ucla.edu.

Staphylococcus aureus is an opportunistic Gram-positive pathogen that causes a wide range of illnesses such as pneumonia, meningitis, endocarditis, toxic shock syndrome, bacteremia, and septicemia (1). Methicillin-resistant *S. aureus* and other drug-resistant strains are a leading cause of life-threatening hospital- and community-acquired infections in the United States (2, 3). *S. aureus* requires iron to proliferate, which it actively procures from its human host during infections (4–7). Heme (protoporphyrin IX + iron) present within hemoglobin (Hb) accounts for ~75–80% of the total iron found in the human body and is preferentially used by *S. aureus* as an iron source (6, 7). Consequently, *S. aureus* and other microbial pathogens have evolved elaborate heme-acquisition systems to exploit this rich iron source. An understanding of the molecular mechanism of heme scavenging will provide insight into how this pathogen survives and persists within its human host, and it could lead to new anti-infective agents that work by limiting microbial access to iron.

S. aureus uses the iron-regulated surface determinant (Isd)[5] system to extract the oxidized form of heme from Hb (hereafter called hemin). The Isd system is composed of nine proteins that form a hemin relay system that captures Hb and rapidly extracts its hemin, transfers hemin across the cell wall, and then pumps the hemin into the cytoplasm where it is degraded to release free iron (8–10). Four Isd proteins (IsdA, IsdB, IsdC, and IsdH/HarA) are covalently linked to the bacterial cell wall via sortase transpeptidases (11, 12). The two surface receptor proteins, IsdH and IsdB, first bind Hb and extract its hemin (13–17). Then the hemin is passed to IsdA, which is partially buried in the cell wall (18). Holo-IsdA subsequently transfers hemin to the fully buried IsdC protein via an ultra-weak handclasp complex (19–22). Finally, holo-IsdC delivers the hemin to the bacterial ABC transporter complex, IsdDEF, which pumps hemin into the cytoplasm where it is degraded to release free iron by the hemin oxygenases, IsdG or IsdI (23, 24). The Isd system is important for *S. aureus* virulence, as strains lacking genes that encode for components of the system display attenuated infec-

[5] The abbreviations used are: Isd, iron-regulated surface determinant; NEAT, NEAr iron Transporter; MD, molecular dynamics; ITC, isothermal titration calorimetry; CV, column volume; AUC, analytical ultracentrifugation; RDF, radial distribution function; IPTG, isopropyl-β-D-thiogalactoside; PDB, Protein Data Bank; Hb, human hemoglobin; Hp, human haptoglobin.

tivity in mouse models and are impaired in their ability to utilize hemin or Hb as the sole source of iron (7, 11, 25–27). Related hemin acquisition systems are used by other Gram-positive pathogens to obtain iron.

Hemin is extracted from the oxidized form of Hb (called methemoglobin) using the *S. aureus* IsdB and IsdH receptors (15, 16, 28–31). The receptors share similar primary sequences and contain NEAr iron Transporter (NEAT) domains, binding modules originally named because they were found in bacterial genes that are proximal to putative Fe^{3+} siderophore transporter genes (32). Our previously published studies of IsdH have shown that it extracts hemin using a tridomain unit formed by its second (N2) and third (N3) NEAT domains, which are connected by a helical linker domain ($IsdH^{N2N3}$, residues Ala-326–Asp-660) (Fig. 1*a*). Studies using native MetHb have shown that $IsdH^{N2N3}$ rapidly extracts hemin from Hb, ~500-fold faster than the rate at which hemin spontaneously dissociates from Hb. Recent NMR and crystallography studies of the Hb-free and -bound forms of IsdH have provided insight into how it promotes hemin release from Hb (29–31). Crystal structures of the Hb·$IsdH^{N2N3}$ complex reveal that the receptor adopts an extended dumbbell-shaped structure in which the N2 domain engages the A- and E-helices of Hb, whereas the N3 domain is positioned within 12 Å of the hemin molecule that is located on the same globin chain (Fig. 1*b*). Hemin release may in part be triggered by the helical linker domain, which distorts the F-helix in Hb that houses the iron-coordinating proximal histidine residue (HF8) (Fig. 1*c*). NMR studies of the apo-receptor uncovered the presence of inter-domain motions between the N2 and linker domains, revealing that the receptor adaptively recognizes Hb. IsdB shares significant primary sequence homology with IsdH and actively acquires hemin from Hb, suggesting that it also employs a semi-flexible tridomain unit to extract Hb's hemin (16, 22, 28, 33).

Although the structural basis of IsdH binding to Hb is now understood, we lack a quantitative understanding of the mechanism of hemin transfer. This is due to the heterogeneous nature of the transfer reaction, which has thus far limited its detailed biophysical characterization. For example, at the concentrations used to monitor hemin release, Hb adopts distinct tetrameric and dimeric quaternary states that have different propensities to release hemin (34, 35). Moreover, IsdH binds to both the α- and β-globin chains within Hb, which also release hemin at different rates (36, 37). Finally, hemin extraction causes Hb to dissociate into its component globin chains, which irreversibly aggregate and release hemin faster than intact Hb (38, 39). Thus, previously measured rates of hemin transfer using WT Hb and IsdH report on an amalgamation of distinct extraction processes, hindering a quantitative understanding of the energetics that underlie hemin extraction. To overcome these limitations, we used a stabilized tetrameric form of Hb and a bacterial receptor mutant that only binds to Hb's α-subunit. By using stopped-flow experiments, we show that the tridomain unit accelerates hemin release from the α-subunit by more than 10,000-fold, a rate that is significantly faster than previously reported values that were measured using heterogeneous components. Transfer requires a Gibbs activation energy of 18.1 ± 1.1 kcal/mol to be surmounted, whose high enthalpic

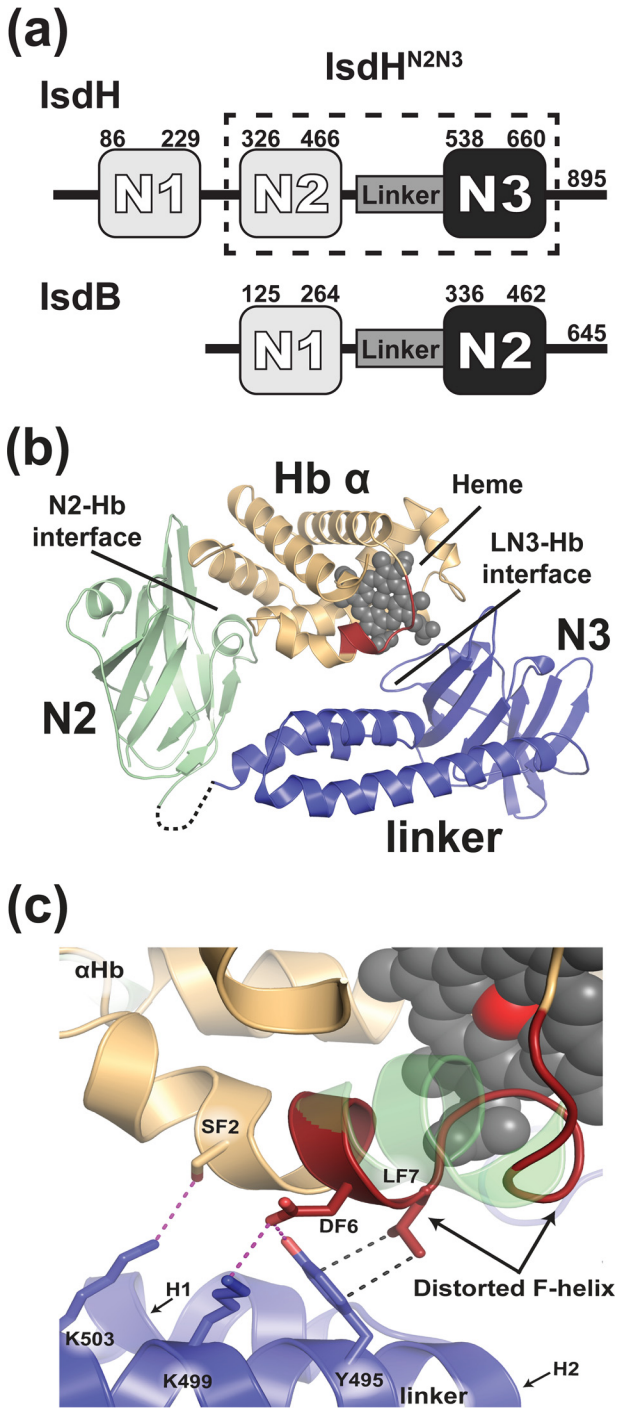

Figure 1. *S. aureus* uses conserved tridomain-containing receptors to capture Hb. *a,* schematic showing the domain organization within the *S. aureus* Hb receptors, IsdH and IsdB. NEAT domains (*N*) that bind Hb and hemin (oxidized form of heme) are shown in *gray* and *black*, respectively. The helical domain that connects them is labeled *linker*. Residue numbers that define the boundaries of the functionally homologous NEAT domains are indicated. *b,* crystal structure of the Hb·α-$IsdH^{N2N3}$ complex (PDB code 4XS0) with only contacts to the α-subunit shown. Proteins are shown in *ribbon* format, and the hemin group is represented by a *space-filling model*. Density for residues in the segment connecting the N2 and linker domains are absent in the electron density (*dashed line*). *c,* close-up view of the LN3·Hb interface that is distorted. α-IsdH is shown in *blue,* and ribbon diagram of αHb is shown in *yellow* (α-IsdH, residues Ala-326–Asp-660 from IsdH containing ^{365}FYHYA^{369} → ^{365}YYHYF^{369} mutations). The F-helix in the receptor·Hb complex that is distorted (*red*) is overlaid with the native F-helix observed in the isolated Hb protein (*green*) (PDB code 2DN2). The hemin group is represented by a *space-filling model* (*gray*) with the iron atom in *red*.

component suggests that in the transition state the proximal histidine–hemin bond (Nϵ–Fe) bond is hydrolytically cleaved. Molecular dynamics (MD) simulations suggest that the receptor's ability to lower the activation energy by ~6 kcal/mol is due to its ability to induce strain in the bond and to increase the concentration of nearby water molecules that compete with Hb's HisF8 Nϵ atom for the iron atom within hemin. Quantitative measurements of Hb-receptor–binding interactions using isothermal titration calorimetry (ITC) indicate that two energetically distinct receptor·Hb interfaces form the pretransfer complex. An interface between the receptor's N2 domain and the A-helix of Hb is the primary contributor to overall binding affinity, tethering IsdH to Hb to enable lower affinity interactions that distort Hb's hemin pocket. A model of the hemin extraction process is presented that incorporates the existing structural kinetics and thermodynamic binding data.

Results

Development of a quantitative assay to study hemin extraction

We developed an assay to quantitatively measure the kinetics of IsdH-mediated hemin removal from the α-globin chain within tetrameric Hb. In the assay, a mutant of $IsdH^{N2N3}$ that only binds to the α-subunit of Hb is used (α-IsdH, residues Ala-326–Asp-660, with ^{365}FYHYA^{369} → ^{365}YYHYF^{369} mutations). α-IsdH contains F365Y and A369F mutations within the α-helix of the Hb-binding N2 domain, which selectively weakens its affinity for the β-subunit in Hb (31). The assay also employs Hb0.1, a tetramer-stabilized recombinant form of Hb in which the two α-subunits are present within a single polypeptide (the C terminus of one α-subunit is joined via a glycine residue to the N terminus of the second α-subunit (40)). Hb0.1 also contains a V1M mutation that facilitates expression in *Escherichia coli* but is otherwise structurally and functionally identical to WT Hb. Because Hb0.1 has a significantly reduced propensity to dissociate into αβ Hb dimers, hemin transfer experiments employing it and α-IsdH enable hemin extraction from the α-globin chain within tetrameric Hb to be selectively monitored (35, 40).

As summarized in Table 1, analytical ultracentrifugation (AUC) sedimentation equilibrium experiments confirm that α-IsdH binds tetrameric Hb0.1 with the appropriate 2:1 stoichiometry via interactions with its α-subunits. In the AUC experiments, to prevent complications caused by hemin transfer, Hb0.1 was maintained in its carbonmonoxy-ligated state, and hemin-binding deficient IsdH proteins were used that contain a Y642A mutation that removes the iron-coordinating tyrosine residue (41). In all AUC experiments, the concentration of Hb0.1 was monitored by measuring its absorbance at 412 nm, the Soret band of the bound heme molecule. As expected, isolated Hb0.1 forms a stable tetramer at concentrations that are used in hemin transfer experiments; at 5 μM (heme units), Hb0.1 has a weighted average molecular mass of 64,212 ± 829 Da at 13,000 × *g*. We next used AUC to determine the Hb0.1·α-$IsdH^{Y642A}$ binding stoichiometry when α-$IsdH^{Y642A}$ is present at a 15-fold molar excess. These data indicate that ~1.8 α-$IsdH^{Y642A}$ proteins bind to each Hb0.1 tetramer, compatible with it only binding to the α-subunits. Increasing the ratio of α-$IsdH^{Y642A}$ to Hb0.1 in the AUC experiments to 30:1 does not increase this stoichiometry, indicating that Hb0.1 is saturated (Fig. 2*a*, *red curve*). In contrast, $IsdH^{Y642A}$, which is identical to α-$IsdH^{Y642A}$ except that it does not contain mutations in the Hb-contacting α-helix, binds to Hb0.1 with a stoichiometry of ~3.2 (Fig. 2*a*, *blue curve*). This is consistent with previous studies that have shown that $IsdH^{Y642A}$ binds to both the α- and β-subunits of Hb (31, 42). To confirm that α-$IsdH^{Y642A}$ interacts with only the α-subunits within Hb0.1, AUC experiments were performed using the β-CO tetramer, which only contains the isolated β-globin protein (Fig. 2*b*). Consistent with previously reported studies, AUC analysis of the β-CO form indicates that it adopts a tetrameric structure: molecular mass of 56,700 ± 724 Da at 6000 × *g* (56,300 ± 508 Da at 13,000 × *g*) (35, 43). When the AUC studies are repeated in the presence of excess $IsdH^{Y642A}$, the receptor binds to the β-CO tetramer with ~2:1 stoichiometry indicating that it can bind to the β-globin chain, but steric effects caused by tetramerization may limit receptor occupancy (molecular mass of 134,000 ± 1321 Da at 6000 × *g*) (Fig. 2*b*, *blue curve*). Interestingly, when similar experiments are performed using α-$IsdH^{Y642A}$, no detectable binding is observed (Fig. 2*b*, *red curve*). Overall, the results of these studies indicate that the α-$IsdH^{Y642A}$ receptor only binds to the α-subunits within Hb0.1 and that both of these subunits are nearly saturated with the receptor at a ratio of 15:1, α-$IsdH^{Y642A}$/Hb0.1 (Hb0.1 concentration 5 μM heme units). These conditions and reagents were therefore used in subsequent stopped-flow hemin transfer experiments to preferentially measure the rate at which the receptor extracts hemin from the α-subunit of tetrameric Hb0.1.

Table 1
Stoichiometry of Hb·receptor complexes determined by analytical ultracentrifugation

	Weighted average molecular masses[a,b]	Receptor/globin
	Da	
Hb0.1[c]		
13,000 × *g*	64,212 ± 829	
Hb0.1 + α-$IsdH^{Y642A}$[c,d]		
6000 × *g*	140,070 ± 2096	2.0
13,000 × *g*	131,570 ± 894	1.7
Hb0.1 + α-$IsdH^{Y642A}$[c,e]		
6000 × *g*	134,660 ± 1,872	1.8
13,000 × *g*	128,490 ± 1115	1.7
Hb0.1 + $IsdH^{Y642A}$[c,e]		
6000 × *g*	188,110 ± 1,518	3.2
13,000 × *g*	175,120 ± 1045	2.9
β-Globin[c]		
6000 × *g*	56,700 ± 724	
13,000 × *g*	56,300 ± 508	
β-Globin + α-$IsdH^{Y642A}$[c,e]		
6000 × *g*	54,500 ± 97	0.0
13,000 × *g*	54,500 ± 65	0.0
β-Globin + $IsdH^{Y642A}$[c,e]		
6000 × *g*	134,000 ± 1321	2.0
13,000 × *g*	116,500 ± 617	1.6

[a] Samples were centrifuged at 25 °C in buffer containing 20 mM sodium phosphate, 150 mM NaCl, 450 mM sucrose, pH 7.5.
[b] Molecular masses were obtained by nonlinear least-squares exponential fitting of data using Beckman Origin-based software (Version 3.01).
[c] Globin chains were held at a concentration of 5 μM (hemin units).
[d] Receptor concentrations were in a 15-fold molar excess (75 μM).
[e] Receptor concentrations were in a 30-fold molar excess (150 μM).

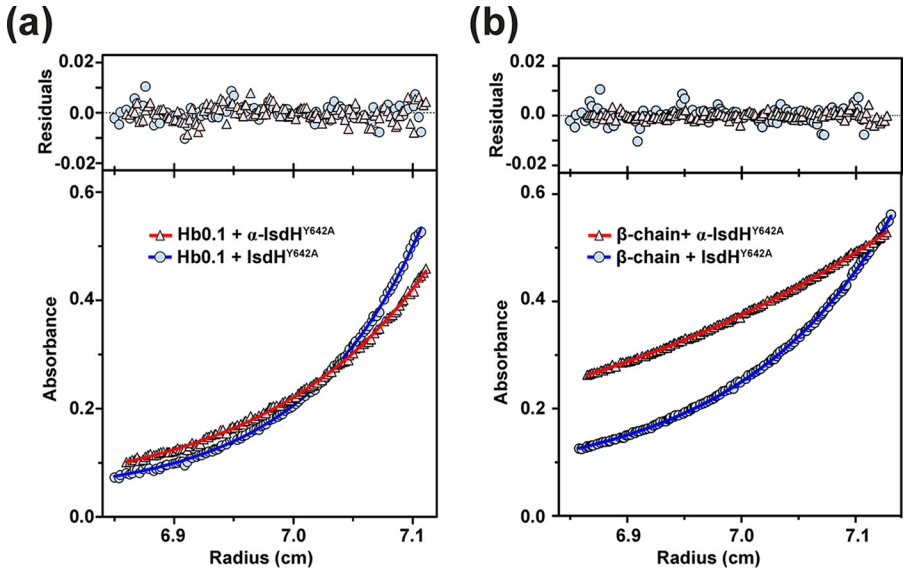

Figure 2. Stoichiometry of Hb·receptor complexes determined by analytical ultracentrifugation. *a,* representative absorbance scans at 412 nm at equilibrium are plotted *versus* the distance from the axis of rotation for a mixture of Hb0.1 + IsdH^{Y642A} (*blue circles*) and Hb0.1 + α-IsdH^{Y642A} (*red triangles*). Hb0.1 was maintained in the carbonmonoxy-ligated state, and both receptors contained the Y642A mutation to prevent heme transfer. Protein samples were mixed at a ratio of 5 μM Hb0.1 and 150 μM receptor and were centrifuged at 25 °C for at least 48 h at 13,000 rpm. The *solid lines* represent the global nonlinear least-squares best fit of all the data to a single molecular species with a baseline fit. Residuals of the fit are shown *above each panel*. *b,* representative scans identical to the conditions described in *a* with the exception that 5 μM β-CO (isolated β-chains) was used, and samples were centrifuged at a speed of 9000 rpm.

Hb tetramerization slows hemin removal from the α-subunit

Stopped-flow UV-visible spectroscopy was used to measure the rate at which α-IsdH extracts hemin from either the stabilized Hb0.1 tetramer or native Hb (results summarized in Table 2). In these experiments, the proteins were rapidly mixed, and the amount of hemin transfer was determined by monitoring UV absorbance changes at 405 nm (29, 35). A 30-fold molar excess of receptor was employed (5 and 150 μM Hb and receptor, respectively) to ensure that α-IsdH saturates the α-globin subunit (Table 1). Upon mixing, a rapid shift in the UV spectrum occurs indicating hemin transfer from Hb0.1 to α-IsdH (Fig. 3*a*). The time-dependent spectral changes exhibit biphasic kinetics, with approximately half of the total magnitude of the spectral change characterized by a rapid event defined by the rate constant k_{fast} and the remaining much slower changes described by k_{slow} (Fig. 3*b*). Importantly, hemin transfer is completed during the time course of the experiment, as minimal additional spectral changes are observed when the proteins are incubated overnight. As the receptor is in excess and has higher affinity for hemin than hemoglobin (described below), we conclude that all of the hemin in Hb0.1 is captured by α-IsdH. The observed pseudo-first– order rate constants, k_{fast} and k_{slow}, are 0.34 ± 0.01 and 0.026 ± 0.001 s^{-1} at 25 °C, respectively. As α-IsdH only binds to the α-subunits of the stabilized Hb0.1 tetramer, we conclude that the rapid changes characterized by k_{fast} describe hemin removal from the α-subunit within tetrameric Hb0.1, whereas the slower changes result from indirect hemin capture from the β-subunit after it has first been released into the solvent. Indirect hemin capture from the β-subunit is consistent with the value of k_{slow}, as it is similar in magnitude to the previously reported rate at which the β-subunit spontaneously releases hemin into solvent from the semihemoglobin form of tetrameric Hb (0.007–0.013 s^{-1}) (35, 39). Moreover, the value of k_{slow} is independent of receptor concentration (Fig. 5*b*). The tetrameric α-subunit spontaneously releases hemin into the solvent at a rate of ~0.000083 s^{-1} at 37 °C. Thus, α-IsdH accelerates the rate of hemin release from the α-subunit ~13,400-fold and scavenges hemin from the β-subunit indirectly via the solvent.

Table 2
Apparent rate constants of hemin transfer

Hemin donor	Hemin acceptor	k_{fast}[a]	k_{slow}[a]
		s^{-1}	s^{-1}
MetHb	α-IsdH[b]	3.27 ± 0.07	0.038 ± 0.001
	IsdH[b]	3.12 ± 0.08	0.039 ± 0.001
	Apo-Mb[c,d]	0.004[e] (0.01)[f]	0.0002[e] (0.003)[f]
MetHb0.1	α-IsdH[b]	0.34 ± 0.01	0.026 ± 0.001
	IsdH[b]	0.73 ± 0.03	0.041 ± 0.001
	Apo-Mb[c,d]	0.0004[g]	0.00008[g]

[a] k_{fast} and k_{slow} values were obtained by fitting to a double-exponential expression.
[b] Rates were determined at a 30-fold excess [receptor], pH 7.5, 25 °C.
[c] Rates were determined at pH 7.0, 37 °C.
[d] The data are from Ref. 35.
[e] k_{fast} and k_{slow} values are from the β- and α-globin chains in dimeric Hb, respectively.
[f] k_{fast} and k_{slow} values are from the β- and α-globin chains in monomeric Hb, respectively.
[g] k_{fast} and k_{slow} values are from the β- and α-globin chains in tetrameric Hb, respectively. These values are also the same for tetrameric wildtype Hb.

To investigate the impact of the dimer-tetramer Hb equilibrium on hemin capture, we measured transfer rates to α-IsdH from Hb, which exists as a mixture of dimeric ($\alpha\beta$) and tetrameric ($\alpha_2\beta_2$) species that have differing propensities to release hemin (35). Stopped-flow experiments indicate that hemin is rapidly removed from Hb, with k_{fast} and k_{slow} rate constants of 3.27 ± 0.07 and 0.041 ± 0.001 s^{-11} at 25 °C, respectively. As for Hb0.1, k_{fast} accounts for approximately half of the overall spectral change that occurs upon receptor mixing with Hb, consistent with it reporting on the rate of hemin removal from the α-subunit. Interestingly, as compared with Hb0.1, the k_{fast} for hemin removal from Hb is increased ~9-fold (Fig. 3*c*). This is

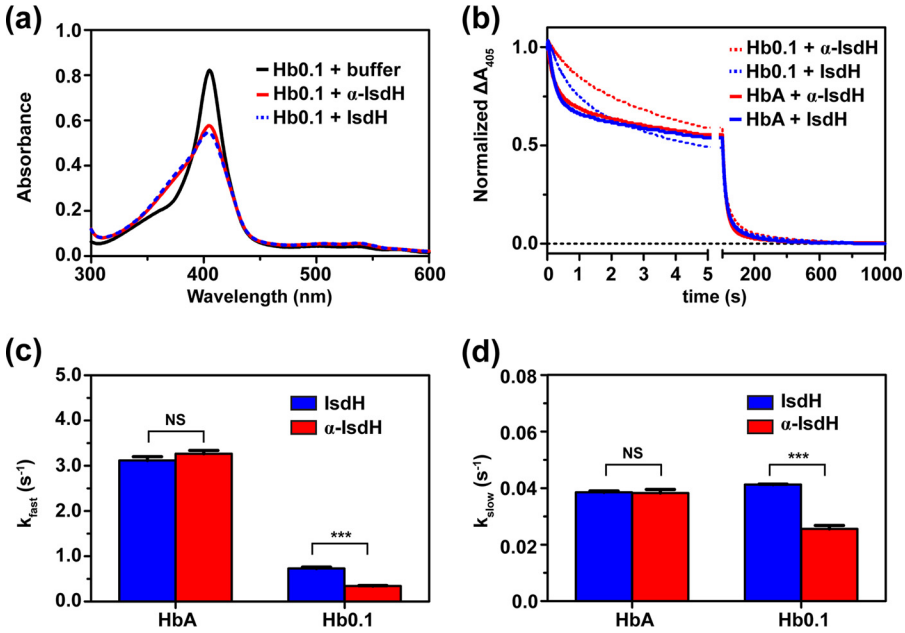

Figure 3. Hemin transfer by various Hb and receptors species. *a,* spectral changes in the UV-visible spectrum of the reaction containing 5 μM Hb0.1 with buffer (*solid black line*), 150 μM IsdH^{N2N3} (*dotted blue line*), and 150 μM α-IsdH (*solid red line*). Spectral traces were recorded at 1000 s post-mixing. *b,* representative stopped-flow time courses showing absorbance changes at 405 nm (ΔA_{405}) after mixing 5 μM Hb or Hb0.1 with 150 μM apo-receptor. The data were fit to a double-exponential equation to obtain k_{fast} and k_{slow} hemin transfer rates. Spectral traces were normalized for comparison using the following equation: $y = (y_t - y_0)/(y_t + y_0)$. *c* and *d* show the measured k_{fast} and k_{slow} rate constants, respectively. Values were derived from the time courses in *b*. A two-way analysis of variance was used to access the significance in the difference of rates. *NS* means not significant (p values >0.05), and *** corresponds to p values <0.001.

consistent with the presence of dimeric species in the reaction containing Hb that are known to release hemin more rapidly than the tetrameric Hb, and the fact that upon hemin removal Hb can fully dissociate into monomeric α-globin chains that have even weaker affinity for hemin (15, 35). More modest 2-fold increases in k_{slow} are also observed when Hb is used instead of Hb0.1 (Fig. 3*d*). They are consistent with the production of isolated β-subunits produced upon Hb dissociation that are known to more rapidly release hemin than tetrameric Hb0.1 (35). However, as this process occurs slowly, α-IsdH presumably extracts hemin from the β-subunits through an indirect process in which the hemin is first released into the solvent.

Hemoglobin tetramer dissociation also accelerates the rate of hemin capture by the native IsdH^{N2N3} receptor that binds to both the α- and β-globin chains. This was demonstrated by measuring the rate of hemin transfer to IsdH^{N2N3} from either Hb or the stabilized Hb0.1 tetramer (Fig. 3*b*). With IsdH^{N2N3}, as with α-IsdH, hemin is removed from Hb0.1 more slowly than it is from Hb, consistent with the reduced propensity of Hb0.1 to dissociate into more labile dimeric and monomeric species upon hemin removal (Fig. 3*c*).

Therefore, the IsdH^{N2N3} receptor's faster kinetics of hemin removal from Hb0.1 may be caused by its ability to also remove hemin from hemoglobin's β-subunit, which is known to release hemin more readily than the α-subunit (35). Combined, these data indicate that the propensity of Hb to dissociate during the extraction process increases the overall observed rate of transfer to the receptor by producing partially hemin-ligated states (semi-forms) or dissociated forms of hemoglobin that have a greater propensity to release their hemin molecules.

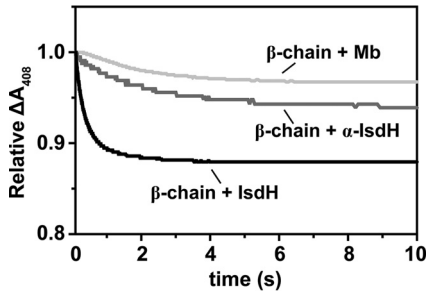

Figure 4. Hemin transfer from isolated β-globin chains. Representative stopped-flow time courses show absorbance changes at 408 nm (ΔA_{408}) after mixing 5 μM isolated Metβ-globin chains with 150 μM apo-receptor or 50 μM apo-Mb. Relative spectral traces are shown for comparison in which all starting absorbances were normalized to a value of 1. Only the first 10 s are shown as absorbance artifacts were observed after this time as a result of the slow process of apo-globin denaturation.

IsdH extracts hemin from both the α- and β-subunits in an effectively irreversible process

The stopped-flow and AUC data indicate that IsdH actively extracts hemin from the α-subunit (Figs. 2 and 3), but it is not known whether the receptor also triggers hemin release from the β-subunit. We therefore probed the ability of IsdH^{N2N3} to remove hemin from tetrameric Metβ, which only contains β-globin chains bound to hemin (Fig. 4). Active removal is observed when IsdH^{N2N3} is added to Metβ, with rapid changes in the absorbance spectrum observed within 5 s of mixing. A detailed interpretation of the kinetics data was not possible because the β-globin chains aggregate after hemin is removed. However, extraction from Metβ occurs at a rate of $\sim$3 s^{-1}, which is similar to the rate at which IsdH^{N2N3} removes hemin from Hb and about 4 times faster than Hb0.1. This is compati-

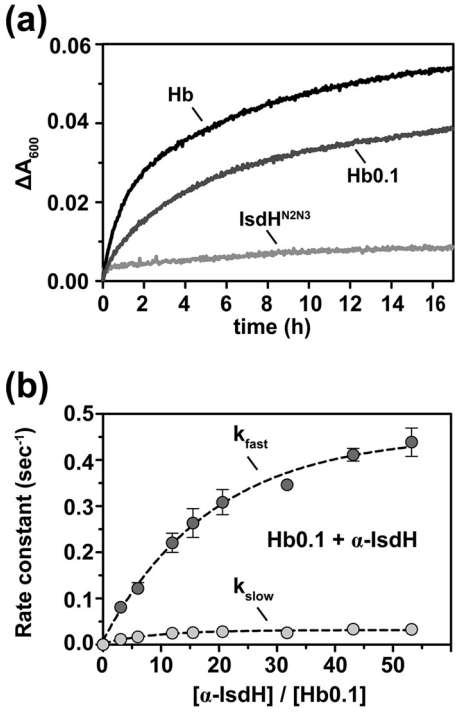

Figure 5. Hemin transfer to myoglobin and as function of receptor concentration. *a,* spontaneous hemin release from the receptor and Hb was measured using H64Y/V68F apomyoglobin. Time courses of the absorbance change at 600 nm (ΔA_{600}) of a mixture of H64Y/V68F apomyoglobin (Mb) with Hb (*black line*), Hb0.1 (*dark gray line*), and IsdH^{N2N3} (*light gray line*) at a final concentration of 50 μM apo-Mb to 5 μM holo-protein. The receptor has higher affinity for hemin as compared with Hb or Hb0.1. *b,* plots of the observed rate constants, k_{fast} (*dark gray circles*) and k_{slow} (*light gray circles*), *versus* the ratio of [α-IsdH] to [Hb0.1]. The concentration of Hb0.1 was held constant at 5 μM. The observed values were obtained in experiments similar to those described in the legend in Fig. 3. For k_{fast}, fits to the data using Equation 1 are shown.

ble with previous studies that have shown that hemin loss from Metβ tetramers is comparable with that of β-subunits within tetrameric Hb (35), and it suggests that IsdH^{N2N3} may remove hemin more rapidly from the β-subunit within Hb than from its α-subunit. In contrast to IsdH^{N2N3}, only modest spectral changes are observed when α-IsdH is added to Metβ (Fig. 4). This is compatible with α-IsdH's inability to bind the β-CO tetramer (Fig. 2*b*), such that it must indirectly scavenge hemin after it has first been released into the solvent. This supported by control transfer studies using recombinant H64Y/V68F apomyoglobin (apo-Mb containing H64Y and V68F mutations), which does not physically interact with Metβ and like α-IsdH slowly scavenges its hemin (Fig. 4) (39). Combined, these results indicate that native IsdH^{N2N3} actively removes hemin from both the α- and β-globin chains within human hemoglobin.

To the best of our knowledge, the relative hemin-binding affinities of IsdH^{N2N3} and Hb have not been reported. We therefore performed hemin-binding competition assays in which each protein was separately mixed with the apo-Mb reagent, which has a known affinity for hemin and whose hemin binding can readily be measured at 600 nm (39). Mixing either 5 μM Hb or Hb0.1 with a 10-fold molar excess of apo-Mb results in a measurable increase in absorbance at 600 nm indicating that hemin is transferred to apo-Mb (Fig. 5*a*). As expected, both transfer processes occur slowly, compatible with hemin first being released into the solvent by hemoglobin before it is subsequently bound by the apo-Mb reagent. These data indicate that apo-Mb has significantly higher affinity for hemin than Hb and Hb0.1. This is compatible with previously reported hemin dissociation constants (K_{-H}) of Hb and apo-Mb; the K_{-H} of apo-Mb is ~0.03 pM, whereas K_{-H} for dimeric Hb is 1.7 and 42 pM for its α and β chains, respectively, and the K_{-H} for tetrameric Hb is 0.8 and 4.2 pM for its α and β chains, respectively (35). Notably, the transfer data reveal that Hb0.1 releases hemin more slowly than Hb (Fig. 5*a*), consistent with previous studies that have shown that the tetrameric form of Hb releases hemin more slowly than the dimeric form (35). In contrast, when hemin containing IsdH^{N2N3} is mixed with the apo-Mb reagent, only small absorbance changes are observed at 600 nm, indicating that unlike Hb and Hb0.1, the receptor has higher affinity for hemin than apo-Mb. Similar to IsdH^{N2N3}, mixing α-IsdH with apo-Mb results in minimal absorbance changes (data not shown). This is expected as mutations in α-IsdH that confer α-globin binding selectivity are located in the N2 domain and are distal to the hemin-binding pocket located in the N3 domain. Taken together, we conclude that IsdH^{N2N3} and α-IsdH bind hemin with K_{-H} values $< \sim 0.03$ pM, such that they have substantially higher affinity for hemin than Hb or Hb0.1. Therefore, during the time frame of the stopped-flow experiments, transfer of hemin from hemoglobin to the receptor is effectively unidirectional and irreversible.

Determination of the micro-rate constants describing hemin removal from the α-subunit

To estimate the micro-rate constants that describe hemin removal, the kinetics data were interpreted using Scheme 1. In this reaction, hemin-bound Hb0.1 first forms a complex with α-IsdH described by the association and dissociation rate constants, k_1 and k_{-1}, respectively. Within the Hb[hemin]·α-IsdH pretransfer complex, hemin is transferred from the α-subunit of tetrameric Hb0.1 to α-IsdH in a process described by k_{trans}. This yields a semi-form of Hb0.1 in which one hemin molecule has been removed, and the protein remains bound to α-IsdH.

$$\text{Hb[hemin]} + {}^{\alpha}\text{IsdH} \underset{k_{-1}}{\overset{k_1}{\rightleftharpoons}} \text{Hb[hemin]:}{}^{\alpha}\text{IsdH} \xrightarrow{k_{trans}} \text{Hb:}{}^{\alpha}\text{IsdH[hemin]}$$

Scheme 1

At the conditions used in our stopped-flow experiments, measured values of k_{fast} describe the kinetics of this entire process and account for the simultaneous removal of hemin from both α-subunits. Contributions to k_{fast} caused by hemin removal from the β-subunit are also possible, but they are expected to be minimal as α-IsdH does not bind to this subunit or actively extract its hemin (Fig. 4 and Table 1). To estimate the micro-rate constants, stopped-flow hemin transfer experiments were performed using varying amounts of α-IsdH in its hemin-free form. At all receptor·Hb0.1 stoichiometries, k_{fast} accounted for ~50% of the total spectral change consistent with it monitoring hemin removal from only the α-subunit (Fig. 3*b*), and the pseudo- first–order values for k_{fast} increased hyperbolically with increasing receptor concentrations (Fig. 5*b*, *dark gray circles*). This is compatible with the rapid formation of a Hb·α-IsdH complex, followed by rate-limiting transfer of hemin to the

receptor. In the transfer experiments (heme-free α-IsdH) is ≥10 (Hb0.1), such that the rate of hemin transfer is pseudo-first–order, and the fraction of pre-transfer complex is small and in steady state during the reaction. The dependence of k_{fast} on the micro-rate constants and receptor concentration can therefore be described by Equation 1 (44),

$$k_{fast} = \frac{k_1 k_{trans}[\alpha - IsdH]}{k_1[\alpha - IsdH] + k_{-1} + k_{trans}} \quad \text{(Eq. 1)}$$

where k_1, k_{-1}, and k_{trans} are the micro-rate constants of the individual reaction steps. As shown in Fig. 5*b*, fitting of the kinetics data using Equation 1 yields values of 2.8×10^7 $M^{-1}\cdot s^{-1}$, 2.4×10^3 s^{-1}, and 0.57 ± 0.02 s^{-1} for k_1, k_{-1}, and k_{trans}, respectively. The fitted value of k_{-1} is much larger than k_{trans}, and as result, only the ratio k_{-1}/k_1 and not the absolute values of these constants are well-defined by the observed data. The equilibrium dissociation constant (K_D) for the Hb0.1·α-IsdH pretransfer complex calculated from the micro-rate constants is 85.7 ± 3.8 μM ($k_{-1}/k_1 = K_D$), a value that is consistent with dissociation constants measured using ITC (described below). The k_{slow} values do not depend on the concentration of the receptor, consistent with it describing absorbance changes caused by hemin release into the solvent from the β-globin chain followed by uptake by α-IsdH (Fig. 5*b*, *light gray circles*).

Enthalpic barrier must be surmounted to capture hemin

Stopped-flow experiments were performed at temperatures ranging from 15 to 37 °C using a molar ratio of 1:40 Hb0.1/α-IsdH (Fig. 6*a*). At this Hb/receptor ratio the contribution of k_{-1}/k_1 to k_{fast} becomes negligible, such that $k_{fast} \approx k_{trans}$ (44). A plot of $\ln(k_{trans}/T)$ *versus* $1/T$ enables the activation parameters to be determined using the linearized form of the Eyring Equation 2,

$$\ln\frac{k}{T} = \ln\left(\frac{k_B}{h}\right) + \frac{\Delta S^{\ddagger}}{R} - \frac{\Delta H^{\ddagger}}{RT} \quad \text{(Eq. 2)}$$

where k_B, h, and R are the Boltzmann, Planck, and ideal gas constants, respectively. The activation enthalpy ($\Delta H^{\ddagger}$) and entropy ($\Delta S^{\ddagger}$) are calculated from slope and intercept, respectively (Fig. 6*b*). This analysis yielded $\Delta H^{\ddagger}$ and $\Delta S^{\ddagger}$ values of 19.45 ± 1.1 kcal/mol and 4.45 ± 0.31 cal/mol·K, respectively, and a $\Delta G^{\ddagger}$ value of 18.07 ± 1.1 kcal/mol at 37 °C. Previous studies have shown that hemin dissociates from the α-globin chain of tetrameric Hb at a rate of 0.000083 s^{-1} (35), which based on the Arrhenius equation indicates that the $\Delta G^{\ddagger}$ for spontaneous hemin release is 23.96 kcal/mol at 37 °C. Thus, the receptor lowers the activation energy needed to release hemin from the α-subunit by ~5.9 kcal/mol, accelerating the rate ~10,000-fold (k_{trans} = 0.88 s^{-1} *versus* 0.000083 s^{-1} at 37 °C).

Two energetically distinct receptor·Hb interfaces are used to bind Hb and distort its hemin pocket

The crystal structure of the Hb·IsdH^{N2N3} complex reveals that the receptor alters the structure of the hemin-binding pocket within Hb, presumably weakening its affinity for hemin (31). Two receptor·Hb interfaces are present in the structure, the N2 domain binds to Hb's A-helix, and the linker and N3

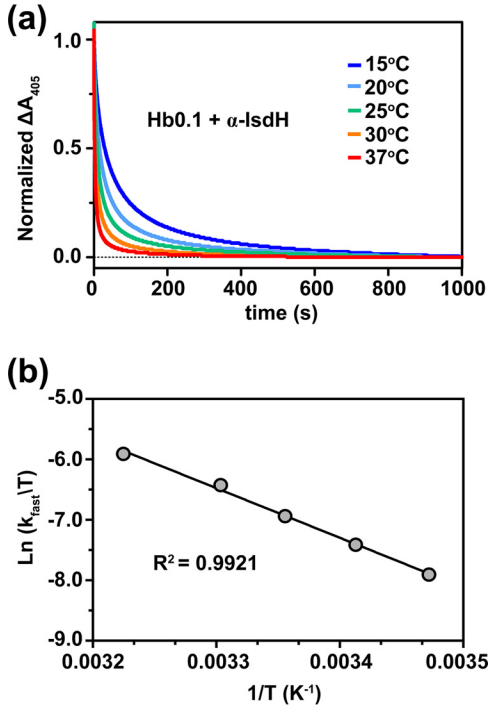

Figure 6. Temperature dependence of hemin transfer. *a*, representative normalized stopped-flow time courses as function of ΔA_{405}. They were obtained by mixing 5 μM Hb0.1 with 200 μM α-IsdH. Spectral traces were normalized using the following equation: $y = (y_t - y_0)/(y_t + y_0)$. *b*, plot of $\ln(k_{fast}/T)$ *versus* $1/T$ is shown. The observed k_{fast} values were obtained in experiments similar to those described in the legend in Fig. 3. The correlation factor, R^2, is indicated on the plot.

domains contact the F-helix within the same globin (Fig. 1*b*). These contact surfaces are extensive, burying 618 and 688 A^2 of surface area, respectively. Previously, we have shown that polypeptides containing only the N2 (IsdH^{N2}) and linker-N3 (IsdH^{LN3}) domains of the receptor are autonomously folded and that IsdH^{LN3} forms a rigid structure (15, 29). Using these protein constructs ITC experiments were performed to gain insight into how each interface contributes to the energetics of Hb binding (Table 3). Initially, binding of α-IsdH^{Y642A} to the carbonmonoxy form of Hb (HbCO) was investigated. As expected, no heme transfer occurs between these proteins when monitored by UV-visible spectroscopy (data not shown) enabling the protein-binding energetics to be quantified. In the ITC experiments, a syringe filled with 200 μM α-IsdH^{Y642A} was injected incrementally into a cell containing 30 μM HbCO, and the ensuing heat changes were used to generate a binding isotherm (Fig. 7*a*). Consistent with the AUC data, α-IsdH^{Y642A} binds Hb at a ratio of ~2:1 (Tables 1 and 3). The measured K_D value for complex is 4.0 ± 0.6 μM and is of similar magnitude as the value obtained from an analysis of the kinetics data. At 25 °C, the standard enthalpy (ΔH^0) and entropy (ΔS^0) of receptor binding are −6.0 ± 0.5 kcal/mol and 4.6 ± 1.9 cal/mol·degrees, respectively (ΔG^0 −7.4 ± 0.1 kcal/mol). To selectively probe binding by the N2 domain, a polypeptide containing only the N2 domain of α-IsdH with the appropriate amino acid mutations that confer binding selectivity for the α-globin chain was studied (α-IsdH^{N2}, residues Ala-326–Pro-466 of α-IsdH). ITC measurements indicate that α-IsdH^{N2} binds HbCO with a K_D of 7.5 ± 1.1 μM and similar ~2:1 stoi-

Table 3
Thermodynamic parameters and affinity data for Hb binding
Errors represent the standard deviation of four replicates.

	K_D	ΔH^0	ΔS^0	ΔG^{0a}	n^b
	μM	*kcal/mol*	*cal/mol·K*	*kcal/mol*	
Hb + αIsdH^{Y642A}	4.0 ± 0.6	−6.0 ± 0.5	4.6 ± 1.9	−7.4 ± 0.1	0.59 ± 0.03
Hb + αIsdH^{N2}	7.5 ± 1.1	−10.3 ± 0.5	−11.1 ± 2.0	−7.0 ± 0.1	0.62 ± 0.04
Hb + αIsdH$^{LN3(Y642A)}$	≥mM	Endothermic	Positive	ND[c]	ND

[a] Samples were in buffer containing 20 mM sodium phosphate, 150 mM NaCl, 450 mM sucrose, pH 7.5, 298 K.
[b] *n* refers to the molar ratio protein/Hb.
[c] ND means not determined.

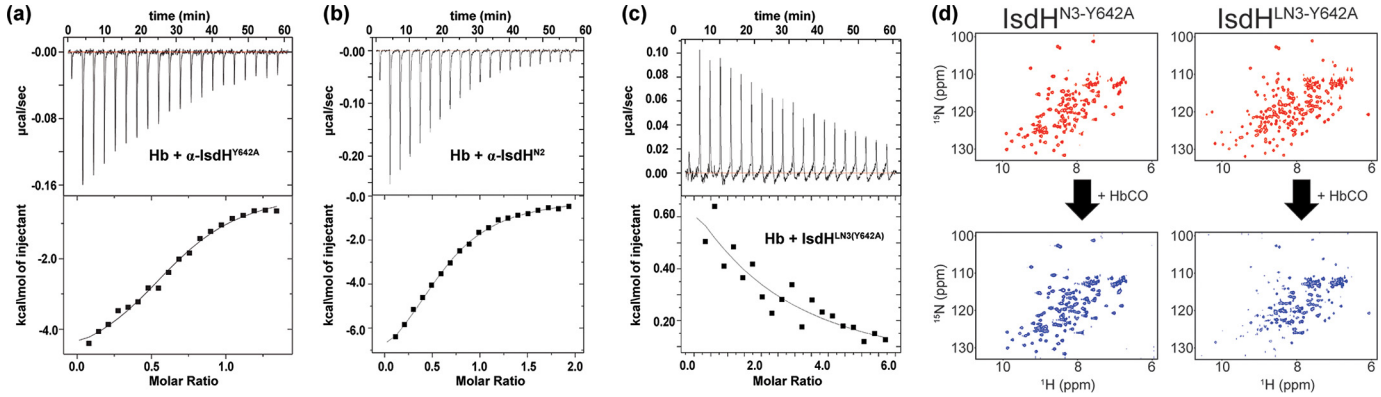

Figure 7. IsdH used two distinct interfaces to promote hemin transfer. *a,* representative ITC data for the titration of 200 μM α-IsdH^{Y642A} into 30 μM HbCO (heme/globin-chain basis). Injections were made at 180-s intervals at 25 °C. *b,* representative ITC data for the titration of 300 μM α-IsdH^{N2} into 30 μM HbCO. *c,* representative ITC data for the titration of 850 μM α-IsdH$^{LN3\text{-}Y642A}$ into 30 μM HbCO. The *top panels* show the time course of the titration (*black*) and baseline (*red*). The *bottom panels* show the integrated isotherms. ORIGIN software was used to fit the data to a single-site binding model to derive thermodynamic parameters. Receptors containing the N3 domain have a Y642A mutation that prevents hemin binding. *d,* NMR titration data showing the effects of Hb binding on ^{15}N-labeled polypeptides that contain only the N3 domain (IsdH$^{N3\text{-}Y642A}$, *left*) or the linker and N3 domains (IsdH$^{LN3\text{-}Y642A}$, *right*). The receptors contain a Y642A mutation that prevents hemin binding. ^{1}H-^{15}N HSQC spectra of the proteins in the absence (*top*) or presence (*bottom*) of a 10-fold excess of HbCO tetramer are shown. Significant peak broadening is only observed when Hb is added to IsdH$^{LN3\text{-}Y642A}$, indicating that linker and N3 domains bind Hb, whereas the N3 domain in isolation does not bind to Hb.

chiometry (Fig. 7*b*). Interestingly, the entropy change associated with HbCO binding is unfavorable for α-IsdH^{N2} (ΔS^0 = −11.1 ± 2.0 kcal/mol·degrees) but favorable for intact α-IsdH^{Y642A}. This difference likely arises from unfavorable ordering of the α-helix within the N2 domain that accompanies Hb binding (30, 45), which, in the context of the longer α-IsdH^{Y642A} protein, is masked by other entropic changes caused by interactions originating from the linker and N3 domains (29, 45).

ITC binding studies were also performed using a polypeptide that contains only the linker and N3 domains of IsdH (IsdH^{LN3}, residues Pro-466–Asp-660, containing a Y642A mutation in the N3 domain to prevent hemin binding). IsdH^{LN3} binds to HbCO, but these interactions are too weak to be accurately quantified. Nevertheless, it is evident from the ITC data that HbCO binding by IsdH^{LN3} is endothermic (Fig. 7*c*), consistent with the crystal structure of the complex that revealed that this portion of the receptor partially unwinds Hb's F-helix. NMR spectroscopy experiments confirm that IsdH^{LN3} and HbCO interact weakly, as cross-peaks in the ^{1}H-^{15}N HSQC spectrum of ^{15}N-enriched IsdH^{LN3} are attenuated and broadened only when large amounts of unlabeled HbCO are added (Fig. 7*d*, *right*). The binding affinity is very weak, with an estimated K_D in the millimolar range. Weak HbCO–IsdH^{LN3} interactions require both the linker and N3 domains in IsdH^{LN3}, as no interactions are observed when HbCO is added to a ^{15}N-enriched IsdH^{N3} polypeptide that only contains the N3 domain (Fig. 7*d*, *left*). Thus, IsdH uses two energetically distinct interfaces to bind Hb. A high-affinity interface formed between the IsdH N2 domain and Hb's A-helix tethers the receptor to Hb, enabling a second, much weaker interface to form in which the F-helix is distorted.

Molecular dynamics simulations reveal the receptor promotes hemin solvation

Hemin release from Hb presumably involves the competitive displacement of the axial histidine Nϵ atom with a water molecule, enabling formation of a new water–Fe^{3+} bond. The observed rate enhancements may therefore in part be due to distortion and increased solvation of the histidine–Fe^{3+} linkage upon receptor binding. To investigate solvation effects of IsdH binding, two explicit solvent 200-ns MD simulations were performed on hemin-containing methemoglobin systems: one with and one without IsdH^{N2N3} bound to the α-subunit (Fig. 8). Over the course of the simulations, the overall complex structures did not exhibit any large-scale structural rearrangements, and the F-helix in the IsdH^{N2N3}-bound structure remained distorted (data not shown). Two analyses were performed to assess the effects of receptor binding on hemin solvation. First, the radial distribution functions (RDFs) of the water hydrogen and oxygen atoms were computed relative to the midpoints of the histidine–iron bonds (Fig. 8*B*). The RDF plots were normalized such that a value of 1.0 is equivalent to bulk solvent. It was observed that in both systems water molecules were allowed to approach this bond; however, in the IsdH^{N2N3}-bound system, the waters were more frequently observed at locations close to

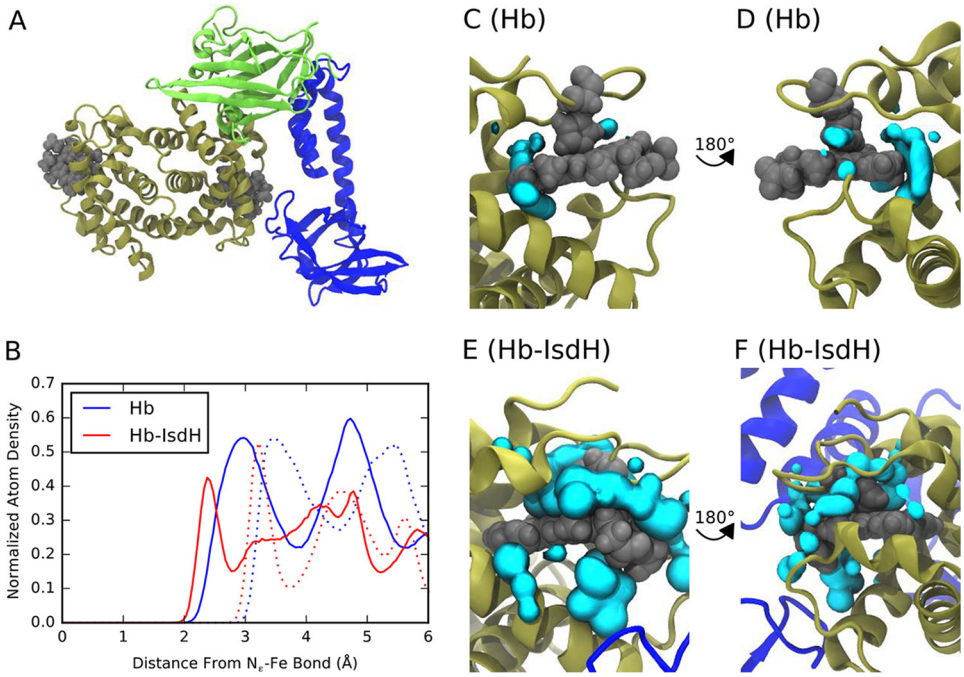

Figure 8. Results of molecular dynamics simulations. *A,* hemoglobin dimer (*gold*) was bound to hemin molecules (*gray*), and an IsdH^{N2N3} molecule (*green* and *blue*) was simulated, along with a system lacking IsdH^{N2N3} (not shown). *B,* radial distribution functions of solvent hydrogen (*solid lines*) and oxygen (*dotted lines*) atoms show that in the receptor-bound system, solvent molecules are more frequently found at closer locations to the Nϵ–Fe bond then in the receptor-free system. Analysis of simulations by a grid inhomogeneous solvation theory analysis showed that in IsdH^{N2N3}-free systems (*C* and *D*) the number of hydration sites (*cyan*) surrounding the hemin group is limited; however, in the IsdH^{N2N3}-bound systems (*E* and *F*) significantly more hydration sites are identified around the Nϵ–Fe bond.

the bond. For example, in the IsdH^{N2N3}-bound system water hydrogens were ~17 times more likely to be located within a distance of 2.1 Å, with the integral of the RDF from 0 to 2.1 Å being 0.016 and 0.001 for the bound and free system, respectively, and hydrogens were ~2 times more likely to be located within 2.5 Å of the bond center.

To further investigate the location and stability of solvent molecules surrounding the iron–nitrogen bond, we performed a grid inhomogeneous solvation theory analysis of our simulations in the region surrounding the receptor-bound hemin. This analysis computes the density, energies, and entropies of water molecules in a three-dimensional grid for the specified region over the equilibrated portion of a simulation. We defined a "hydration site" as a position in space in which the occupancies of water oxygen molecules were at least three times greater than water in bulk, and which the estimated free energies of water molecules were less than zero relative to bulk. This definition effectively chooses locations where it is favorable for a water molecule to occupy relative to being in the bulk, which is accounted for by both a thermodynamic analysis as well as an observed high occupancy. Results of this analysis show that in both the IsdH^{N2N3}-free and -bound forms of Hb, hydration sites exist within the heme-binding pocket. However, when IsdH^{N2N3} binds to Hb, more of these hydration sites occur near the axial His-87 residue in Hb (compare Fig. 8, *C* and *E*). Combined with the RDF analysis, these data indicate that the hemin pocket in Hb is never completely devoid of water molecules and show that when IsdH binds to Hb closer and more stable hydration occurs near atoms that are proximal to the iron–nitrogen covalent bond. We conclude that receptor-introduced distortions in the axial bond that weaken its affinity, combined with increased solvation, favor water in the competitive displacement equilibrium.

Discussion

S. aureus acquires iron from human hemoglobin using two related surface receptors, IsdH and IsdB (46). The receptors extract Hb's hemin using a conserved tridomain unit that is formed by two NEAT domains that are separated by a helix linker domain (Fig. 1*a*) (15). The mechanism of extraction is best understood for IsdH. Previously, we have shown that the NEAT domains within its tridomain unit (IsdH^{N2N3}) synergistically extract hemin from Hb at a rate that is significantly faster than the rate at which Hb spontaneously releases hemin into the solvent. A 4.2 Å resolution crystal structure of the Hb·IsdH^{N2N3} complex revealed that each receptor engages a single globin chain, with the N2 domain contacting the globin's A-helix and the N3 domain positioned near its hemin molecule (30). The hemin needs to slide only ~12 Å from the globin into the receptor's N3 domain where its iron atom is coordinated by a tyrosine residue. A subsequently higher resolution 2.55 Å structure of the complex contained the receptor bound to the α-globin and revealed it may trigger hemin release by distorting the F-helix that contains the axial histidine residue (HisF8) (31). Although atomic structures have provided great insight into the process of hemin extraction, the energetics underling this process are poorly understood. This is because the native IsdH-Hb system is heterogeneous, as Hb exists in dimeric and tetrameric forms that have different propensities to release hemin, and once hemin is removed from Hb it dissociates into its component globins that aggregate and more rapidly release hemin. Furthermore, our stopped-flow results indicate

IsdH^{N2N3} extracts hemin from both the α- and β-subunits within Hb (Figs. 3 and 4) and that the native IsdH binds to tetrameric Hb with sub-saturating stoichiometry (Table 1). Thus, the heterogeneous properties of the native system limit its detailed biophysical characterization.

To quantitatively analyze hemin extraction from Hb, we developed an assay that preferentially monitors hemin transfer from only its α-subunit. This was accomplished by using a stabilized tetramer of Hb (Hb0.1) and a variant of IsdH^{N2N3} (α-IsdH) that we show only binds to the α-subunit (Table 1). Stopped-flow UV-visible experiments reveal that α-IsdH captures hemin in a biphasic manner; a rapid phase characterized by k_{fast} describes the active extraction of hemin from the α-globin subunit, whereas slower spectral changes defined by the k_{slow} report on the indirect capture of hemin from the β-subunits after it has first been released into the solvent. The latter conclusion is supported by our finding that the k_{slow} values are independent of α-IsdH concentration (Fig. 5*b*).

It is possible that some rapid, activated hemin transfer occurs from β-subunits and contributes to the fast phase in the IsdH^{N2N3} experiments because our spectral and kinetic measurements do not distinguish between these subunits. The notion of accelerated heme dissociation from Hb β-subunits is suggested by the results of AUC and hemin transfer experiments, both of which indicate that IsdH^{N2N3} binds to isolated Metβ subunits and rapidly acquires its hemin. However, the amplitude of the fast phase is 50% in the transfer experiments with both α-IsdH, where only α chains interact with the receptor and IsdH^{N2N3}, where some binding to β-subunits does occur. This result implies that the fast phase represents activated heme transfer from α-subunits in both cases. However, it is conceivable that hemin release from the β-subunit also contributes passively to k_{fast}, as our spectral and kinetic measurements cannot distinguish easily between these subunits. Additional experiments using valence hybrid mutants of Hb are required to fully resolve this issue (39).

Our results suggest that the receptor removes hemin at a faster rate from dimeric MetHb ($\alpha\beta$) than it does from tetrameric MetHb ($\alpha_2\beta_2$), as α-IsdH removes hemin 10-fold faster from native Hb than it does from Hb0.1 (k_{fast} 0.34 and 3.27 s^{-1}, respectively) (Table 2 and Fig. 3*c*). This conclusion is supported by our AUC data that indicate that Hb0.1 adopts a tetrameric state at the concentrations used in our stopped-flow studies (Table 1), whereas Hb is a mixture of dimeric and tetrameric forms; at the 5 μM hemoglobin concentrations used in this study, ~65% of Hb is tetrameric and ~35% dimeric ($K_{4,2}$ of 1.5 μM) (35). The larger k_{fast} for native Hb is presumably caused by hemin removal from its dimeric form, which is known to release hemin more rapidly than the tetramer (35). ESI-MS studies have also shown that hemin removal by the receptor causes native Hb to dissociate into its monomeric globin chains (15). This latter process further explains why α-IsdH removes hemin more rapidly from Hb than from Hb0.1, as the isolated globins caused by native Hb dissolution release hemin at faster rates than Hb dimers and tetramers (35). Similar effects are observed for IsdH^{N2N3}, which, like α-IsdH, removes hemin more rapidly from native Hb than it does from the stabilized Hb0.1 tetramer. Interestingly, when the k_{fast} values for hemin removal from Hb0.1 are compared, IsdH^{N2N3} removes hemin ~2-fold faster than α-IsdH (Fig. 3*c*). We speculate that this difference is caused by the IsdH^{N2N3} receptor's unique ability to also extract hemin from the β-subunit of Hb0.1, which has weaker affinity for hemin than the α-subunit. This notion is substantiated by the results of AUC and hemin transfer experiments that indicate that IsdH^{N2N3} binds to Metβ and rapidly acquires its hemin. The measured k_{fast} for hemin transfer from Hb0.1 to IsdH^{N2N3} is therefore likely an amalgam of the rates of hemin removal from both types of globin chains within hemoglobin, whereas the k_{fast} of transfer to α-IsdH only reflects hemin removal from the α-globin that binds hemin more tightly. No differences in k_{fast} are observed between the receptors when Hb is employed as the hemin donor, as tetramer dissociation accelerates hemin release thereby masking subtle globin-specific contributions to k_{fast} (Fig. 3*b*). These complications highlight the benefits of using Hb0.1 and α-IsdH to selectively monitor hemin removal, as the native receptor captures hemin from both globins in a process that is facilitated by Hb dissociation into its component monomeric globins and dimeric Hb (Table 2).

The micro-rate constants and energetics of hemin extraction were estimated using data from the α-specific transfer assay. Extraction can be envisioned as occurring through Scheme 1, with the ratio of k_{-1}/k_1 describing the equilibrium dissociation constant for formation of the Hb·α·IsdH complex, and k_{trans} representing the process that moves hemin from Hb into the receptor. Transfer is essentially unidirectional, as competition studies with apoMb indicate that IsdH^{N2N3} binds hemin with significantly higher affinity than Hb (Fig. 5*a*). Fitting of these data yielded values of 85.7 ± 3.8 μM and 0.57 ± 0.02 s^{-1} for k_{-1}/k_1 and k_{trans}, respectively (Fig. 5). The value of k_{trans} is ~60% larger than the measured value of k_{fast}, presumably because Hb is only partially saturated with the receptor at the protein concentrations used in the transfer assay. An Eyring plot of the temperature dependence of k_{trans} reveals that hemin transfer is limited by an enthalpic barrier at 37 °C, with $\Delta G^{\ddagger}$ = 18.1 ± 1.1 kcal/mol, and $\Delta H^{\ddagger}$ and $\Delta S^{\ddagger}$ values of 19.5 ± 1.1 kcal/mol. The activation energy required for spontaneous hemin release from the α-subunit of tetrameric Hb is ~24 kcal/mol (47). Thus, α-IsdH effectively lowers $\Delta G^{\ddagger}$ by ~6 kcal/mol, consistent with the ~10,000-fold rate enhancement observed in our hemin transfer experiments as compared with the rate of spontaneous hemin release from Hb.

We hypothesize that breakage of the HisF8-iron is rate-limiting in the hemin transfer reaction and that it occurs through a displacement mechanism in which a water molecule outcompetes HisF8 as a ligand for the Fe(III) atom within hemin (48). The Hb·IsdH^{N2N3} crystal structure may resemble the pretransfer complex (Scheme 1), because the hemin in this structure remains bound to Hb via a HisF8 –iron bond. After bond breakage, the mostly nonpolar hemin would then travel ~12 Å through a predominantly hydrophobic pathway to the receptor's N3 domain to form the post-transfer complex (Scheme 1) (31). In the Hb·IsdH^{N2N3} crystal structure, the receptor unwinds the F-helix, which may lower the energy required to break the axial bond breakage by inducing strain. Receptor-induced pocket distortions could also lower the activation

energy by increasing the concentration of water molecules near the bond, increasing the probability that they can outcompete HisF8's Nϵ atom for hemin's iron atom. Indeed, our MD simulations reveal that receptor binding to Hb causes more stable and closer hydration to occur near the axial bond, perhaps favoring water in the competitive displacement equilibria (Fig. 8). Similar hydration of the space near the Fe–HisF8 bond was clearly observed in the crystal structure of the L89(F8)G mutant of Mb, which showed a similar 3000-fold increase in the rate of hemin dissociation at pH 7 (48).

The MD simulations also suggest that the receptor alters the positioning of the HisF8 –iron bond, but its quantitative impact on axial bond strength will require the application of more sophisticated computational methods. Interestingly, altering the conformation of the F-helix may be a general strategy used to modulate Hb's hemin affinity, as helical fluctuations in globin chains have been shown to govern overall affinity (38, 49–53). Moreover, this strategy is employed by the α-Hb–stabilizing protein, which promotes autooxidation of α-globin chains by binding to a distal site that causes localized distortions in the F-helix (54–56).

Receptor-hemoglobin binding measurements employing ITC reveal that IsdH^{N2N3} uses two energetically distinct binding interfaces with Hb to form the pretransfer complex (Table 3). The first interface is composed of the N2 domain that binds to the A- and E-helices of Hb (N2·Hb interface), whereas the second interface contains the linker and N3 domains that interact with F-helix and EF- and FG-corners of Hb (LN3·Hb interface) (Fig. 1*b*). Using receptor truncation mutants, we demonstrated that the N2·Hb interface drives formation of the pretransfer complex. This is evident from our finding that the IsdH^{N2} polypeptide binds to Hb with similar affinity as the intact tridomain receptor IsdH^{N2N3}, K_D = 7.5 ± 1.1 and 4.0 ± 0.6 μM, respectively (Table 3). Conversely, the LN3·Hb interface that contains the distorted F-helix forms with very weak affinity as judged by ITC and NMR (K_D >1 mM). ITC data indicate that unwinding Hb's F-helix is enthalpically unfavorable, as IsdH^{LN3} binding to Hb causes heat to be absorbed (Fig. 7), a comparison of the binding data for α-IsdH and α-IsdH^{N2} reveals less favorable ΔH^0 changes occur for the intact α-IsdH receptor as compared with α-IsdH^{N2} (ΔH^0 = −6.0 ± 0.5 and −10.3 ± 0.5 kcal/mol for α-IsdH and α-IsdH^{N2}, respectively) (Table 3). In contrast, formation of the higher affinity N2·Hb interface causes favorable enthalpic changes and unfavorable changes in binding entropy (ΔS^0 = −11.0 ± 2 cal/mol·K). The latter effect is likely caused by ordering of loop 2, which undergoes a disordered-to-ordered transition upon binding Hb's A helix (30, 42, 45). Thus, despite burying similar solvent-exposed surface areas, the N2·Hb interface is the primary determinant for overall binding affinity, whereas the LN3·Hb interface forms with very weak affinity because of the large enthalpic penalty that must be paid to distort Hb's F-helix. Recently, binding of IsdH to the Hb·Hp complex was studied by surface plasmon resonance, and it was reported that native IsdH^{N2N3} binds Hb-Hp with a K_D ~ 120 nM (57), which is an order of magnitude higher in affinity than our ITC measured affinity of the Hb·IsdH^{N2N3} complex. This difference may result from the distinct methods that were employed. However, it is interesting to note that both the IsdH^{N1} domain and IsdB have been reported to bind the Hb·Hp complex with higher affinity than Hb alone (58). As these receptors do not contact Hp directly, it is possible that subtle Hp-induced changes in the structure of Hb may increase its binding affinity for IsdH and IsdB. However, remarkably Hp binding prevents hemin transfer from Hb to IsdB in the ternary complex (57). Thus, the Hp-induced conformational changes prevent hemin dissociation with and without bound receptor (59).

Our measured binding energetics for α-IsdH are generally similar to those previously reported for IsdB^{N1N2}, which is the analogous tridomain unit within IsdB (33). Nevertheless, there are clear differences. Most notably, IsdB^{N1N2} was reported to bind HbCO with 10-fold higher affinity than IsdH^{N2N3}, and unlike IsdH^{N2} that binds Hb with high affinity, the analogous isolated domain from IsdB (IsdB^{N1}) binds HbCO with weak affinity. Thus, despite a high degree of sequence homology shared by the two receptors, there may be significant biochemical differences whose molecular basis needs to be deciphered.

Our studies enable a free energy reaction coordinate diagram to be constructed that describes the process of receptor-mediated hemin extraction from the α-subunit of Hb (Fig. 9). Prior to engaging Hb, the IsdH^{N2N3} receptor undergoes interdomain motions in which the position of the N2 domain moves with respect to the linker and N3 domains that form a rigid unit (29). In step 1, the higher affinity N2·Hb interface forms (ΔG^0 = −7.0 ± 0.1 kcal/mol), contributing ~95% of the total binding standard free energy for the receptor·Hb complex. In step 2, the much weaker Hb·LN3 interface forms, unraveling the F-helix to form the pretransfer complex in a process that is enthalpically unfavorable. It is unclear whether Hb binding quenches N2·LN3 inter-domain motions within the receptor. In principle, the two distinct receptor·Hb binding interfaces could form in a concerted manner, with binding at the higher affinity N2·Hb interface nucleating new receptor inter-domain and Hb–receptor interactions that immobilize the receptor on Hb and drive formation of the lower affinity Hb·LN3 interface. However, in the crystal structure of the Hb·IsdH^{N2N3} complex, no significant N2–linker interdomain interactions are observed, and electron density for residues Asn-465–Glu-472 connecting these domains is poorly resolved. Thus, it is possible that inter-domain motions at the N2·Hb interface persist after Hb·IsdH^{N2N3} complex formation, with the N2·Hb interface holding the mobile LN3 unit near Hb's hemin to increase its effective molarity and the likelihood of forming weak contacts to Hb in which the F-helix is unwound (60). Persistent receptor inter-domain motions within the Hb·IsdH^{N2N3} complex may also facilitate downstream hemin transfer from IsdH to IsdA, because, in principle, they would not be reliant upon the complete dissociation of the complex. In step 3, Hb's hemin molecule is transferred to IsdH following a 12-Å path that is exposed to the solvent. Transfer requires a Gibbs activation energy of 18.1 ± 1.1 kcal/mol to be surmounted. We hypothesize that this energy is needed to hydrolytically cleave the proximal histidine– hemin bond (Nϵ–Fe) bond, as $\Delta H^{\ddagger}$ is 19.5 ± 1.1 kcal/mol. The structure of the complex and our MD simulations suggest that the receptor lowers the activation energy by ~6 kcal/mol by inducing strain in the bond and by increasing the

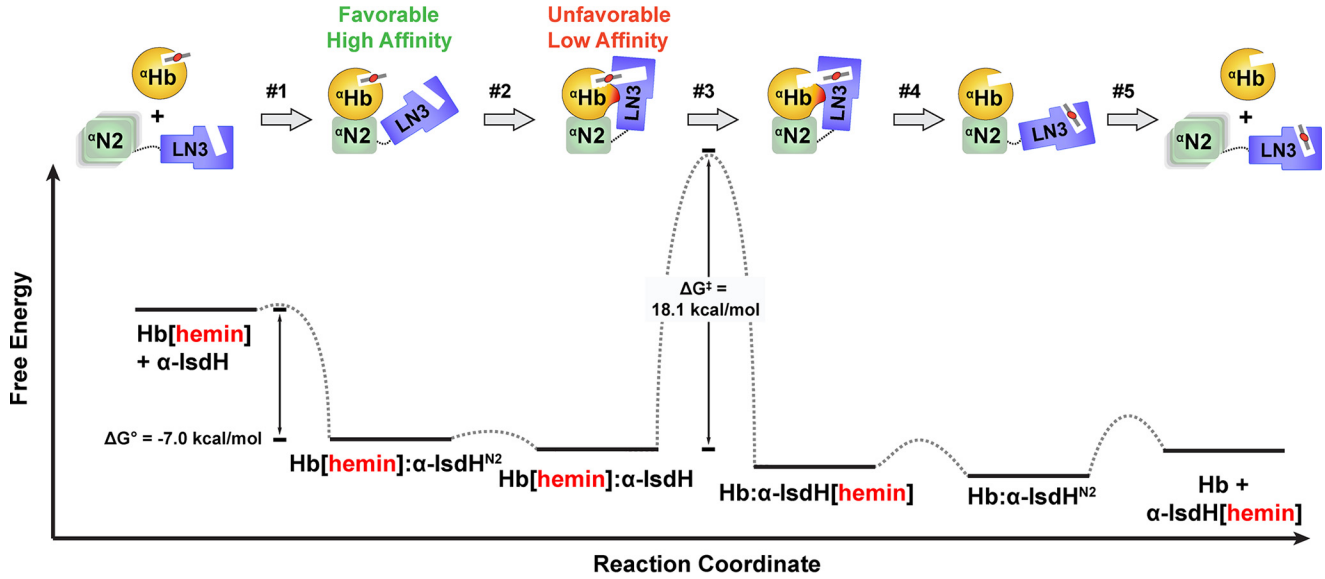

Figure 9. Model of the hemin extraction mechanism. Shown is a proposed hemin transfer reaction coordinate diagram. The IsdH^{N2N3} receptor recognizes Hb via two energetically distinct interfaces (N2·Hb and LN3·Hb interfaces). *Top,* schematic showing the steps in hemin transfer. *Bottom,* relative free energies of the intermediates. Free energies calculated from this study are labeled along reaction coordinate diagram. Breakage of the axial Fe–Nϵ bond is presumably rate-limiting (step 3). The following color scheme was used: N2, *green*; linker-N3, *blue*; Hb α-subunit, *gold*.

concentration of nearby water molecules that compete with HisF8's Nϵ atom for the iron atom within hemin. Based on studies of spontaneous hemin release from Mb and Hb, bond breakage may be facilitated by formation of a hemichrome (61). Indeed, a bis·His hemin complex has recently been observed in the structure of the IsdB·Hb complex (62). The receptor likely extracts hemin from the β-subunit using a similar mechanism, but the energetics of this process remain ill-defined. Once hemin is transferred, the hemin-bound receptor dissociates from Hb, presumably through the two-step process in which the weaker Hb·LN3 interface disengages first (step 4), followed by dissociation of the stronger Hb·N2 interface (step 5). The structure of the post-hemin transfer complex is not known, so it is possible that hemin transfer to the N3 domain alters its structure further weakening the Hb·LN3 interface. Transfer is effectively unidirectional as IsdH binds hemin with significantly higher affinity than Hb based on competition studies with apo-Mb.

Hemin removal by the native receptor from WT Hb is expected to be significantly more complex and could involve simultaneous removal from both the α- and β-subunits, as well as receptor-induced dissociation of Hb into dimeric and monomeric species. Based on unfolding studies with purified Hbs, receptor-mediated hemin removal from WT Hb could cause the formation of a dimeric molten globular intermediate in which the α1β1 interface remains intact, but the heme pocket has partially melted, facilitating the hemin removal from both subunits (63). However, in our structure of the complex, only the αF-helix has unfolded. Although we now have an idea about the mechanism and energies that underlie hemin transfer from the α-subunit, it remains unknown how hemin moves between the proteins, how interdomain motions affect this process, and whether there are true mechanistic differences between IsdH and IsdB. The new assay we describe in this paper could be a valuable tool to help answer these questions.

Experimental procedures

Cloning and protein preparation

IsdH proteins were expressed from pET-28b–based plasmids and initially contained a removable N-terminal hexahistidine–small-ubiquitin-like modifier (SUMO) tag to facilitate purification (pHis-SUMO) (64, 65). Protein-expressing plasmids include the following: pRM208 encoding Ala-326–Asp-660 in IsdH (IsdH^{N2N3}); pRM216 encoding Ala-326–Asp-660 that contains a Y642A substitution (IsdH^{N2N3}-Y642A); pMMS322 encoding Ala-326–Asp-660 with substitution of ^{365}FYHYA^{369} → ^{365}YYHYF^{369} that confers selectivity for the α-globin chain of Hb (α-IsdH^{N2N3}); and pMMS323 containing the same substitution of ^{365}FYHYA^{369} → ^{365}YYHYF^{369} as well as a Y642A substitution (α-IsdH^{N2N3}-Y642A) (15, 31, 66). In addition, the pET-28b–based plasmid pSUMO-Mb was constructed that expresses recombinant sperm whale myoglobin H64Y/V68F with a removable SUMO tag (Mb$^{H64Y/V68F}$). The expression plasmids were constructed using standard approaches and made use of the QuickChange site-directed mutagenesis kit, (Stratagene, La Jolla, CA). The proteins were expressed by transforming the aforementioned plasmids into *Escherichia coli* BL21-DE3 cells (New England Biolabs, Beverly, MA). Protein expression and purification procedures have been described previously (15). Briefly, expression proceeded overnight at 25 °C by adding 1 mM isopropyl-β-D-thiogalactoside (IPTG) to cell cultures. The bacterial cells were then harvested by centrifugation and lysed by sonication, and the protein was purified using a Co^{2+}-chelating column (Thermo Fisher Scientific, Waltham, MA). The N-terminal His_6-SUMO tag was then cleaved using the ULP1 protease, and mixture was reapplied to the Co^{2+}-chelating column to remove the protease and cleaved SUMO tag. The hemin-free forms for the IsdH and Mb proteins were generated by hemin extraction with methyl ethyl ketone followed by buffer exchange into 20 mM NaH_2PO_4, 150 mM

NaCl, pH 7.5 (67). Hemin-saturated proteins were produced by adding a 1.5 M excess of hemin to purified protein solutions followed by removal of excess hemin using a Sephadex G-25 column (GE Healthcare) equilibrated with 20 mM Tris-HCl, pH 8.0. Protein·hemin stoichiometries were determined using UV-visible spectroscopy and calculating the A_{Soret}/A_{280}.

Human hemoglobin was prepared as described previously from the blood of a healthy donor provided by the CFAR Virology Core Lab at the UCLA AIDS Institute (68). Briefly, red blood cells were washed in 0.9% NaCl solution and then lysed under hypotonic conditions. Hb was purified from the hemolysate by two ion-exchange chromatography steps, cation-exchange (SP-Sepharose, GE Healthcare), followed by anion-exchange chromatography (Q-Sepharose, GE Healthcare). During the purification, the globin chains were maintained in the carbon monoxide-liganded state to inhibit autooxidation and subsequent denaturation. Recombinant genetically stabilized human hemoglobin was expressed from plasmid pSGE1.1-E4 in *E. coli* BL21-DE3 cells and contains V1M mutations in both α- and β-globin chains and a glycine linker between the C terminus of one α-subunit and the N terminus of another α-subunit (called Hb0.1) (40, 69). Cells were grown in M9 minimal media containing 3 g/liter glucose and 1 g/liter NH_4Cl as the sole source of carbon and nitrogen, respectively. Prior to induction, exogenous hemin was added to the cell cultures to a final concentration of 8 μM. Expression was performed at 16 °C overnight by adding IPTG to cell cultures to achieve a final concentration of 1 mM. Cells were then harvested by centrifugation, and washed with lysis buffer (50 mM Tris-HCl, 17 mM NaCl, pH 8.5) twice to remove excess hemin. The cell suspension was then purged with a steady stream of CO for 15 min in an ice-water bath. All buffers used during the purification were kept at pH 8.5 and were purged with CO to prevent heme oxidation. The cells containing recombinant Hb0.1 were lysed by sonication and purified in a single step using a Co^{2+}-chelating column (Thermo Fisher Scientific) via interactions with the naturally occurring His residues on the surface of Hb0.1. The column was washed using three buffers prior to elution with imidazole: 5 volumes (CV) of lysis buffer (see above), 5 CVs of wash buffer 1 (20 mM Tris-HCl, 500 mM NaCl, pH 8.5), and 5 CVs of wash buffer 2 (20 mM Tris-HCl, pH 8.5). Column-bound Hb was then eluted with 5 CVs of elution buffer (20 mM Tris-HCl, 100 mM imidazole, pH 8.5).

Hemin transfer experiments

Ferric Hb and Hb0.1 (methemoglobin) were used in the hemin transfer experiments. They were produced by converting the carbonmonoxy form of each pure protein into the ferric form using established methods and described for Hb. Briefly, HbCO was converted into HbO_2 by delivering a pure stream of oxygen gas over HbCO solution kept cold in an ice-water bath and simultaneously illuminated with a high-intensity (100 watts) light source. Removal of CO from HbCO and conversion to HbO_2 was considered complete when the ratio of A_{577}/A_{560} was ~1.8 (70). Oxidation of HbO_2 to generate ferric Hb was achieved by incubating HbO_2 with a 5-fold molar excess of potassium ferricyanide followed by application of the sample to a Sephadex G-25 column (GE Healthcare) to remove the excess ferricyanide. Ferric Hb (or Hb0.1) was then buffer exchanged into 20 mM NaH_2PO_4, 150 mM NaCl, pH 7.5. The concentration of hemin within each form of the protein was determined using the extinction coefficient of 179 mM^{-1} cm^{-1} at a wavelength of 405 nm (71).

The kinetics of hemin transfer from ferric Hb (donor) to apo-IsdH proteins (acceptor) were measured using an Applied Photophysics SX18.MV stopped-flow spectrophotometer (Applied Photophysics, Surrey, UK). Acceptor and donor proteins were dissolved in 20 mM NaH_2PO_4, 150 mM NaCl, pH 7.5, supplemented with 0.45 M sucrose to prevent absorbance changes caused by apoprotein aggregation (39). Ferric Hb was mixed with apo-acceptor present at ≥10 M excess (in hemin units) to maintain pseudo-first– order conditions. After rapid mixing (dead-time 3 ms), absorbance changes at 405 nm were monitored for 1000 s. Experiments were performed in triplicate, and the data were analyzed by fitting the observed time courses to a double-phase exponential expression using the GraphPad Prism program (GraphPad Software, version 5.01). As described here, micro-rate constants describing the hemin transfer were obtained by fitting the dependence of the observed fast-phase kinetic rate constant (k_{fast}) on the concentration of apo-receptor (Equation 1) using Mathematica software (Wolfram Mathematica 9.0, Wolfram Research). For slower transfer reactions involving apo-$Mb^{H64Y/V68F}$ (39), a 10-fold molar excess of apo-$Mb^{H64Y/V68F}$ was used, and absorbance changes were measured using a conventional UV-visible spectrophotometer. For these reactions, the entire UV-visible spectrum was recorded over a 17-h period.

Analytical ultracentrifugation

Sedimentation equilibrium runs were performed at 25 °C in a Beckman Optima XL-A analytical ultracentrifuge using absorption optics at 412 nm so that only the heme molecule was detected. The protein concentrations in samples analyzed by AUC were the same as those used for the stopped-flow hemin transfer experiments (20 mM sodium phosphate, 150 mM NaCl, 0.45 M sucrose, pH 7.5). To limit hemin transfer during the AUC experiment, IsdH proteins contained the Y642A mutation that limits heme binding, and the carbon monoxide-liganded form of Hb0.1 (or β-Hb) was used to limit heme release. Three-mm pathlength double sector cells were used for all samples, and were purged with CO before sealing the cells to prevent oxidation. Sedimentation equilibrium profiles were measured at speeds of 9000 (~6000 × *g*) and 13,000 rpm (~13,000 × *g*). Samples contained Hb0.1 or β-Hb (isolated β-globin chains) at a concentration of 5 μM and 0, 75, and 150 μM α-$IsdH^{Y642A}$. Experiments using native $IsdH^{Y642A}$ made use of a 150 μM sample. Weight-average molecular masses were determined by fitting with a nonlinear least-squares exponential fit for a single ideal species using the Beckman Origin-based software (version 3.01). Partial specific volumes were calculated from the amino acid compositions and corrected to 25 °C (72, 73). They were 0.749 for the αβ Hb heterodimer and β-globin chains, 0.735 for apo-receptor, and 0.739 for the complex. At higher concentrations of receptor, the fitted molecular weights were slightly lower than those obtained when lower receptor concentrations were used, which is compatible with the increased nonideality of the solution.

Isothermal titration calorimetry

ITC measurements were performed using a MicroCal iTC200 calorimeter (GE Healthcare) at 25 °C. To prevent heat changes due to hemin transfer, the Hb was maintained in the carbonmonoxy-ligated state and hemin-binding deficient receptor proteins containing an alanine substitution for Tyr-642. The HbCO and the apo-receptor proteins were buffer-matched in ITC buffer (20 mM NaH_2PO_4, 150 mM NaCl, 0.45 M sucrose, pH 7.5). The cell was filled with 30 μM HbCO, and the syringe was filled with 200, 300, and 850 μM α-$IsdH^{Y642A}$, α-$IsdH^{N2}$, $IsdH^{LN3(Y642A)}$, respectively. Twenty injections were performed using 2.0-μl injection volumes at 180-s intervals. ORIGIN software was used to fit the data to a single-site binding model. The heat (Q) is related to the number of sites (n), the binding constant (K), and the enthalpy (ΔH) via Equation 3,

$$Q = \frac{nM_t\Delta HV_o}{2}\left(1 + \frac{X_t}{nM_t} + \frac{1}{nKM_t} - \sqrt{\left(1 + \frac{X_t}{nM_t} + \frac{1}{nKM_t}\right)^2 - \frac{4X_t}{nM_t}}\right) \quad \text{(Eq. 3)}$$

where X_t, M_t, and V_o represent the bulk concentration of ligand, the bulk concentration of macromolecule in V_o, and the active cell volume, respectively. A correction is made to account for the displaced volume after the ith injection, as shown in Equation 4,

$$\Delta Q(i) = Q(i) + \frac{dV_i}{V_o}\left(\frac{Q(i) + Q(i-1)}{2}\right) - Q(i-1) \quad \text{(Eq. 4)}$$

Calculated $\Delta Q(i)$ values for each injection are compared with the corresponding experimental values. The fit is improved over successive iterations by altering values for n, K, and ΔH (74).

Molecular dynamic simulations

The protein structure for the IsdH-bound system was taken directly from a methemoglobin dimer·IsdH complex (PDB code 4XS0, resolution 2.55 Å (31)), and the coordinates of native methemoglobin were taken from a tetramer deoxy-hemoglobin structure (PDB code 1A3N, resolution 1.8 Å (75)). Missing residues in each structure were added using ModLoop (76). Both systems were neutralized with Na^+ ions and solvated with TIP3P (77) waters and a 150 mM NaCl environment in a periodic box, which had a minimum of 10 Å from protein heavy atoms to the box edge. Following minimization for 4500 steps, both systems were heated to 300 K with restraints of 10 kcal/mol/$Å^2$ on the solute heavy atoms applied for 20 ps, and the restraints were then gradually removed over 350 ps. Production simulations of 200 ns were then performed in the NPT ensemble with temperature maintained via a Langevin thermostat and pressure-regulated with a Berendsen barostat (78). Nonbonded interactions were truncated at 10 Å, and long ranged electrostatics were computed with the particle-mesh Ewald method using a maximum spacing of 1.0 Å. All simulations were performed with the GPU accelerated version of PMEMD in the Amber16 package (79). The AMBERff14SB force field was used for the proteins, whereas parameters for hemin and the Nϵ–Fe^{3+} bond were calculated following the protocol of Shahrokh *et al.* (80). In short, geometry optimization, frequency calculations, and electrostatic potential calculations were done in Gaussian09 (81), and a RESP fit was performed in antechamber Gaussian, and tleap scripts were generated using MCBP.py from AmberTools16. Bonded and van der Waals parameters were derived from the General Amber Force Field (82). Analysis of each system was performed on the final 150 ns of simulations using visual molecular dynamics (83), MDAnalysis (84), and CPPTRAJ (85). The grid inhomogeneous solvation theory analysis was done with a grid spanning 33 × 41 × 61 Å and a grid spacing of 0.5 Å.

Author contributions—M. S., R. M., and R. T. C. conceptualization; M. S., R. M., J. D. M., J. C., J. S. O., J. W., and R. T. C. data curation; M. S., R. M., J. D. M., J. C., J. S. O., M. L. P., D. A. G., J. W., and R. T. C. formal analysis; M. S., R. M., J. D. M., J. C., J. S. O., J. W., and R. T. C. investigation; M. S., R. M., J. D. M., and R. T. C. writing-original draft; J. S. O., M. L. P., D. A. G., and J. W. resources; J. S. O., M. L. P., J. W., and R. T. C. supervision; J. S. O., M. L. P., D. A. G., J. W., and R. T. C. validation; M. L. P. and D. A. G. software; J. W. and R. T. C. methodology; R. T. C. funding acquisition; R. T. C. project administration.

Acknowledgments—We thank Dr. Robert Peterson for assistance with the NMR experiments. NMR equipment used in this research was purchased using funds from shared Equipment Grant National Institutes of Health S10OD016336.

References

1. Klevens, R. M., Morrison, M. A., Nadle, J., Petit, S., Gershman, K., Ray, S., Harrison, L. H., Lynfield, R., Dumyati, G., Townes, J. M., Craig, A. S., Zell, E. R., Fosheim, G. E., McDougal, L. K., Carey, R. B., *et al.* (2007) Invasive methicillin-resistant *Staphylococcus aureus* infections in the United States. *JAMA* **298,** 1763–1771 CrossRef Medline
2. Centers for Disease Control and Prevention (2013) Active Bacterial Core Surveillance (ABCs) Report Emerging Infections Program Network Methicillin-Resistant *Staphylococcus aureus*, Atlanta, GA
3. Dukic, V. M., Lauderdale, D. S., Wilder, J., Daum, R. S., and David, M. Z. (2013) Epidemics of community-associated methicillin-resistant *Staphylococcus aureus* in the United States: a meta-analysis. *PLoS ONE* **8,** e52722 CrossRef Medline
4. Ong, S. T., Ho, J. Z., Ho, B., and Ding, J. L. (2006) Iron-withholding strategy in innate immunity. *Immunobiology* **211,** 295–314 CrossRef Medline
5. Haley, K. P., and Skaar, E. P. (2012) A battle for iron: host sequestration and *Staphylococcus aureus* acquisition. *Microbes Infect.* **14,** 217–227 CrossRef Medline
6. Farrand, A. J., Reniere, M. L., Ingmer, H., Frees, D., and Skaar, E. P. (2013) Regulation of host hemoglobin binding by the *Staphylococcus aureus* Clp proteolytic system. *J. Bacteriol.* **195,** 5041–5050 CrossRef Medline
7. Skaar, E. P., Humayun, M., Bae, T., DeBord, K. L., and Schneewind, O. (2004) Iron-source preference of *Staphylococcus aureus* infections. *Science* **305,** 1626–1628 CrossRef Medline
8. Mazmanian, S. K., Skaar, E. P., Gaspar, A. H., Humayun, M., Gornicki, P., Jelenska, J., Joachmiak, A., Missiakas, D. M., and Schneewind, O. (2003) Passage of heme-iron across the envelope of *Staphylococcus aureus*. *Science* **299,** 906–909 CrossRef Medline
9. Maresso, A. W., and Schneewind, O. (2006) Iron acquisition and transport in *Staphylococcus aureus*. *Biometals* **19,** 193–203 CrossRef Medline
10. Reniere, M. L., Torres, V. J., and Skaar, E. P. (2007) Intracellular metalloporphyrin metabolism in *Staphylococcus aureus*. *Biometals* **20,** 333–345 CrossRef Medline

11. Mazmanian, S. K., Ton-That, H., Su, K., and Schneewind, O. (2002) An iron-regulated sortase anchors a class of surface protein during *Staphylococcus aureus* pathogenesis. *Proc. Natl. Acad. Sci. U.S.A.* **99,** 2293–2298 CrossRef Medline
12. Ton-That, H., Marraffini, L. A., and Schneewind, O. (2004) Protein sorting to the cell wall envelope of Gram-positive bacteria. *Biochim. Biophys. Acta* **1694,** 269–278 CrossRef Medline
13. Pilpa, R. M., Robson, S. A., Villareal, V. A., Wong, M. L., Phillips, M., and Clubb, R. T. (2009) Functionally distinct NEAT (NEAr Transporter) domains within the *Staphylococcus aureus* IsdH/HarA protein extract heme from methemoglobin. *J. Biol. Chem.* **284,** 1166–1176 CrossRef Medline
14. Pishchany, G., Sheldon, J. R., Dickson, C. F., Alam, M. T., Read, T. D., Gell, D. A., Heinrichs, D. E., and Skaar, E. P. (2014) IsdB-dependent hemoglobin binding is required for acquisition of heme by *Staphylococcus aureus*. *J. Infect. Dis.* **209,** 1764–1772 CrossRef Medline
15. Spirig, T., Malmirchegini, G. R., Zhang, J., Robson, S. A., Sjodt, M., Liu, M., Krishna Kumar, K., Dickson, C. F., Gell, D. A., Lei, B., and Loo, J. A., Clubb, R. T. (2013) *Staphylococcus aureus* uses a novel multidomain receptor to break apart human hemoglobin and steal its heme. *J. Biol. Chem.* **288,** 1065–1078 CrossRef Medline
16. Zhu, H., Li, D., Liu, M., Copié, V., and Lei, B. (2014) Non-heme-binding domains and segments of the *Staphylococcus aureus* IsdB protein critically contribute to the kinetics and equilibrium of heme acquisition from methemoglobin. *PLoS ONE* **9,** e100744 CrossRef Medline
17. Dryla, A., Gelbmann, D., von Gabain, A., and Nagy, E. (2003) Identification of a novel iron regulated staphylococcal surface protein with haptoglobin-haemoglobin binding activity. *Mol. Microbiol.* **49,** 37–53 CrossRef Medline
18. Pishchany, G., Dickey, S. E., and Skaar, E. P. (2009) Subcellular localization of the *Staphylococcus aureus* heme iron transport components IsdA and IsdB. *Infect. Immun.* **77,** 2624–2634 CrossRef Medline
19. Villareal, V. A., Spirig, T., Robson, S. A., Liu, M., Lei, B., and Clubb, R. T. (2011) Transient weak protein-protein complexes transfer heme across the cell wall of *Staphylococcus aureus*. *J. Am. Chem. Soc.* **133,** 14176–14179 CrossRef Medline
20. Abe, R., Caaveiro, J. M., Kozuka-Hata, H., Oyama, M., and Tsumoto, K. (2012) Mapping ultra-weak protein-protein interactions between heme transporters of *Staphylococcus aureus*. *J. Biol. Chem.* **287,** 16477–16487 CrossRef Medline
21. Muryoi, N., Tiedemann, M. T., Pluym, M., Cheung, J., Heinrichs, D. E., and Stillman, M. J. (2008) Demonstration of the iron-regulated surface determinant (Isd) heme transfer pathway in *Staphylococcus aureus*. *J. Biol. Chem.* **283,** 28125–28136 CrossRef Medline
22. Zhu, H., Xie, G., Liu, M., Olson, J. S., Fabian, M., Dooley, D. M., and Lei, B. (2008) Pathway for heme uptake from human methemoglobin by the iron-regulated surface determinants system of *Staphylococcus aureus*. *J. Biol. Chem.* **283,** 18450–18460 CrossRef Medline
23. Matsui, T., Nambu, S., Ono, Y., Goulding, C. W., Tsumoto, K., and Ikeda-Saito, M. (2013) Heme degradation by *Staphylococcus aureus* IsdG and IsdI liberates formaldehyde rather than carbon monoxide. *Biochemistry* **52,** 3025–3027 CrossRef Medline
24. Reniere, M. L., Ukpabi, G. N., Harry, S. R., Stec, D. F., Krull, R., Wright, D. W., Bachmann, B. O., Murphy, M. E., and Skaar, E. P. (2010) The IsdG-family of haem oxygenases degrades haem to a novel chromophore. *Mol. Microbiol.* **75,** 1529–1538 CrossRef Medline
25. Torres, V. J., Pishchany, G., Humayun, M., Schneewind, O., and Skaar, E. P. (2006) *Staphylococcus aureus* IsdB is a hemoglobin receptor required for heme iron utilization. *J. Bacteriol.* **188,** 8421–8429 CrossRef Medline
26. Pishchany, G., McCoy, A. L., Torres, V. J., Krause, J. C., Crowe, J. E., Jr., Fabry, M. E., and Skaar, E. P. (2010) Specificity for human hemoglobin enhances *Staphylococcus aureus* infection. *Cell Host Microbe* **8,** 544–550 CrossRef Medline
27. Kim, H. K., DeDent, A., Cheng, A. G., McAdow, M., Bagnoli, F., Missiakas, D. M., and Schneewind, O. (2010) IsdA and IsdB antibodies protect mice against *Staphylococcus aureus* abscess formation and lethal challenge. *Vaccine* **28,** 6382–6392 CrossRef Medline
28. Fonner, B. A., Tripet, B. P., Eilers, B. J., Stanisich, J., Sullivan-Springhetti, R. K., Moore, R., Liu, M., Lei, B., and Copié, V. (2014) Solution structure and molecular determinants of hemoglobin binding of the first NEAT domain of IsdB in *Staphylococcus aureus*. *Biochemistry* **53,** 3922–3933 CrossRef Medline
29. Sjodt, M., Macdonald, R., Spirig, T., Chan, A. H., Dickson, C. F., Fabian, M., Olson, J. S., Gell, D. A., and Clubb, R. T. (2016) The PRE-derived NMR model of the 38.8-kDa tri-domain IsdH protein from *Staphylococcus aureus* suggests that it adaptively recognizes human hemoglobin. *J. Mol. Biol.* **428,** 1107–1129 CrossRef Medline
30. Dickson, C. F., Kumar, K. K., Jacques, D. A., Malmirchegini, G. R., Spirig, T., Mackay, J. P., Clubb, R. T., Guss, J. M., and Gell, D. A. (2014) Structure of the hemoglobin-IsdH complex reveals the molecular basis of iron capture by *Staphylococcus aureus*. *J. Biol. Chem.* **289,** 6728–6738 CrossRef Medline
31. Dickson, C. F., Jacques, D. A., Clubb, R. T., Guss, J. M., and Gell, D. A. (2015) The structure of haemoglobin bound to the haemoglobin receptor IsdH from *Staphylococcus aureus* shows disruption of the native α-globin haem pocket. *Acta Crystallogr. D Biol. Crystallogr.* **71,** 1295–1306 CrossRef Medline
32. Andrade, M. A., Ciccarelli, F. D., Perez-Iratxeta, C., and Bork, P. (2002) NEAT: a domain duplicated in genes near the components of a putative Fe^{3+} siderophore transporter from Gram-positive pathogenic bacteria. *Genome Biol.* **3,** RESEARCH0047 Medline
33. Bowden, C. F., Verstraete, M. M., Eltis, L. D., and Murphy, M. E. (2014) Hemoglobin binding and catalytic heme extraction by IsdB NEAT domains. *Biochemistry* **53,** 2286–2294 CrossRef Medline
34. Benesch, R. E., and Kwong, S. (1995) Coupled reactions in hemoglobin. Heme-globin and dimer-dimer association. *J. Biol. Chem.* **270,** 13785–13786 CrossRef Medline
35. Hargrove, M. S., Whitaker, T., Olson, J. S., Vali, R. J., and Mathews, A. J. (1997) Quaternary structure regulates hemin dissociation from human hemoglobin. *J. Biol. Chem.* **272,** 17385–17389 CrossRef Medline
36. Bunn, H. F., and Jandl, J. H. (1968) Exchange of heme among hemoglobins and between hemoglobin and albumin. *J. Biol. Chem.* **243,** 465–475 Medline
37. Gattoni, M., Boffi, A., Sarti, P., and Chiancone, E. (1996) Stability of the heme-globin linkage in $\alpha\beta$ dimers and isolated chains of human hemoglobin. A study of the heme transfer reaction from the immobilized proteins to albumin. *J. Biol. Chem.* **271,** 10130–10136 CrossRef Medline
38. Leutzinger, Y., and Beychok, S. (1981) Kinetics and mechanism of heme-induced refolding of human α-globin. *Proc. Natl. Acad. Sci. U.S.A.* **78,** 780–784 CrossRef Medline
39. Hargrove, M. S., Singleton, E. W., Quillin, M. L., Ortiz, L. A., Phillips, G. N., Jr., Olson, J. S., and Mathews, A. J. (1994) His64(E7)→Tyr apomyoglobin as a reagent for measuring rates of hemin dissociation. *J. Biol. Chem.* **269,** 4207–4214 Medline
40. Looker, D., Abbott-Brown, D., Cozart, P., Durfee, S., Hoffman, S., Mathews, A. J., Miller-Roehrich, J., Shoemaker, S., Trimble, S., Fermi, G., *et al.* (1992) A human recombinant haemoglobin designed for use as a blood substitute. *Nature* **356,** 258–260 CrossRef Medline
41. Watanabe, M., Tanaka, Y., Suenaga, A., Kuroda, M., Yao, M., Watanabe, N., Arisaka, F., Ohta, T., Tanaka, I., and Tsumoto, K. (2008) Structural basis for multimeric heme complexation through a specific protein-heme interaction: the case of the third neat domain of IsdH from *Staphylococcus aureus*. *J. Biol. Chem.* **283,** 28649–28659 CrossRef Medline
42. Krishna Kumar, K., Jacques, D. A., Pishchany, G., Caradoc-Davies, T., Spirig, T., Malmirchegini, G. R., Langley, D. B., Dickson, C. F., Mackay, J. P., Clubb, R. T., Skaar, E. P., Guss, J. M., and Gell, D. A. (2011) Structural basis for hemoglobin capture by *Staphylococcus aureus* cell-surface protein, IsdH. *J. Biol. Chem.* **286,** 38439–38447 CrossRef Medline
43. McGovern, P., Reisberg, P., and Olson, J. S. (1976) Aggregation of deoxyhemoglobin subunits. *J. Biol. Chem.* **251,** 7871–7879 Medline
44. Espenson, J. H. (1995) *Chemical Kinetics and Reaction Mechanisms*, McGraw-Hill, New York
45. Pilpa, R. M., Fadeev, E. A., Villareal, V. A., Wong, M. L., Phillips, M., and Clubb, R. T. (2006) Solution structure of the NEAT (NEAr Transporter) domain from IsdH/HarA: the human hemoglobin receptor in *Staphylococcus aureus*. *J. Mol. Biol.* **360,** 435–447 CrossRef Medline

46. Sheldon, J. R., and Heinrichs, D. E. (2015) Recent developments in understanding the iron acquisition strategies of gram positive pathogens. *FEMS Microbiol. Rev.* **39,** 592–630 CrossRef Medline
47. Perutz, M. F. (1979) Regulation of oxygen affinity of hemoglobin: influence of structure of the globin on the heme iron. *Annu. Rev. Biochem.* **48,** 327–386 CrossRef Medline
48. Liong, E. C., Dou, Y., Scott, E. E., Olson, J. S., and Phillips, G. N. (2001) Waterproofing the heme pocket. Role of proximal amino acid side chains in preventing hemin loss from myoglobin. *J. Biol. Chem.* **276,** 9093–9100 CrossRef Medline
49. Hargrove, M. S., Barrick, D., and Olson, J. S. (1996) The association rate constant for heme binding to globin is independent of protein structure. *Biochemistry* **35,** 11293–11299 CrossRef Medline
50. Rose, M. Y., and Olson, J. S. (1983) The kinetic mechanism of heme binding to human apohemoglobin. *J. Biol. Chem.* **258,** 4298–4303 Medline
51. Makowski, L., Bardhan, J., Gore, D., Lal, J., Mandava, S., Park, S., Rodi, D. J., Ho, N. T., Ho, C., and Fischetti, R. F. (2011) WAXS studies of the structural diversity of hemoglobin in solution. *J. Mol. Biol.* **408,** 909–921 CrossRef Medline
52. Abaturov, L. V., Nosova, N. G., Shliapnikov, S. V., and Faĭzullin, D. A. (2006) The conformational dynamic of the tetramer hemoglobin molecule as revealed by hydrogen exchange. I. Influence pH, temperature and ligand binding. *Mol. Biol.* **40,** 326–340 Medline
53. Kawamura-Konishi, Y., Chiba, K., Kihara, H., and Suzuki, H. (1992) Kinetics of the reconstitution of hemoglobin from semihemoglobins α and β with heme. *Eur. Biophys. J.* **21,** 85–92 Medline
54. Dickson, C. F., Rich, A. M., D'Avigdor, W. M., Collins, D. A., Lowry, J. A., Mollan, T. L., Khandros, E., Olson, J. S., Weiss, M. J., Mackay, J. P., Lay, P. A., and Gell, D. A. (2013) α-Hemoglobin-stabilizing protein (AHSP) perturbs the proximal heme pocket of oxy-α-hemoglobin and weakens the iron-oxygen bond. *J. Biol. Chem.* **288,** 19986–20001 CrossRef Medline
55. Krishna Kumar, K., Dickson, C. F., Weiss, M. J., Mackay, J. P., and Gell, D. A. (2010) AHSP (α-haemoglobin-stabilizing protein) stabilizes apo-α-haemoglobin in a partially folded state. *Biochem. J.* **432,** 275–282 CrossRef Medline
56. Zhou, S., Olson, J. S., Fabian, M., Weiss, M. J., and Gow, A. J. (2006) Biochemical fates of α hemoglobin bound to α hemoglobin-stabilizing protein AHSP. *J. Biol. Chem.* **281,** 32611–32618 CrossRef Medline
57. Sæderup, K. L., Stødkilde, K., Graversen, J. H., Dickson, C. F., Etzerodt, A., Hansen, S. W., Fago, A., Gell, D., Andersen, C. B., and Moestrup, S. K. (2016) The *Staphylococcus aureus* protein IsdH inhibits host hemoglobin scavenging to promote heme acquisition by the pathogen. *J. Biol. Chem.* **291,** 23989–23998 CrossRef Medline
58. Dryla, A., Hoffmann, B., Gelbmann, D., Giefing, C., Hanner, M., Meinke, A., Anderson, A. S., Koppensteiner, W., Konrat, R., von Gabain, A., and Nagy, E. (2007) High-affinity binding of the staphylococcal HarA protein to haptoglobin and hemoglobin involves a domain with an antiparallel eight-stranded β-barrel fold. *J. Bacteriol.* **189,** 254–264 CrossRef Medline
59. Mollan, T. L., Jia, Y., Banerjee, S., Wu, G., Kreulen, R. T., Tsai, A. L., Olson, J. S., Crumbliss, A. L., and Alayash, A. I. (2014) Redox properties of human hemoglobin in complex with fractionated dimeric and polymeric human haptoglobin. *Free Radic. Biol. Med.* **69,** 265–277 CrossRef Medline
60. Krishnamurthy, V. M., Semetey, V., Bracher, P. J., Shen, N., and Whitesides, G. M. (2007) Dependence of effective molarity on linker length for an intramolecular protein-ligand system. *J. Am. Chem. Soc.* **129,** 1312–1320 CrossRef Medline
61. Harrington, J. P., Newton, P., Crumpton, T., and Keaton, L. (1993) Induced hemichrome formation of methemoglobins A, S and F by fatty acids, alkyl ureas and urea. *Int. J. Biochem.* **25,** 665–670 CrossRef Medline
62. Bowden, C. F. M., Chan, A. C. K., Li, E. J. W., Arrieta, A. L., Eltis, L. D., and Murphy, M. E. P. (2018) Structure-function analyses reveal key features in *Staphylococcus aureus* IsdB-associated unfolding of the heme-binding pocket of human hemoglobin. *J. Biol. Chem.* **293,** 177–190 CrossRef Medline
63. Samuel, P. P., Ou, W. C., Phillips, G. N., Jr., and Olson, J. S. (2017) Mechanism of human apohemoglobin unfolding. *Biochemistry* **56,** 1444–1459 CrossRef Medline
64. Senturia, R., Faller, M., Yin, S., Loo, J. A., Cascio, D., Sawaya, M. R., Hwang, D., Clubb, R. T., and Guo, F. (2010) Structure of the dimerization domain of DiGeorge critical region 8. *Protein Sci.* **19,** 1354–1365 CrossRef Medline
65. Reverter, D., and Lima, C. D. (2004) A basis for SUMO protease specificity provided by analysis of human Senp2 and a Senp2-SUMO complex. *Structure* **12,** 1519–1531 CrossRef Medline
66. Spirig, T., and Clubb, R. T. (2012) Backbone (1)H, (13)C and (15)N resonance assignments of the 39 kDa staphylococcal hemoglobin receptor IsdH. *Biomol. NMR Assign.* **6,** 169–172 CrossRef Medline
67. Ascoli, F., Fanelli, M. R., and Antonini, E. (1981) Preparation and properties of apohemoglobin and reconstituted hemoglobins. *Methods Enzymol.* **76,** 72–87 CrossRef Medline
68. Gell, D., Kong, Y., Eaton, S. A., Weiss, M. J., and Mackay, J. P. (2002) Biophysical characterization of the α-globin binding protein α-hemoglobin stabilizing protein. *J. Biol. Chem.* **277,** 40602–40609 CrossRef Medline
69. Looker, D., Mathews, A. J., Neway, J. O., and Stetler, G. L. (1994) Expression of recombinant human hemoglobin in *Escherichia coli*. *Methods Enzymol.* **231,** 364–374 CrossRef Medline
70. Manning, J. M. (1981) [14] Preparation of hemoglobin carbamylated at specific NH2-terminal residues. *Methods Enzymol.* **76,** 159–167 CrossRef Medline
71. Antonini, E., and Brunori, M. (1971) *Hemoglobin and Myoglobin in their Reactions with Ligands*, North Holland Publishing Co., Amsterdam
72. Cohn, E. J., and Edsall, J. T. (1943) in *Proteins, Amino Acids and Peptides as Ions and Dipolar Ions* (Cohn, E. J., and Edsall, J. T., eds), pp. 713–714, Reinhold Publishing Corp., New York
73. Laue, T., Shah, B., Ridgeway, T., and Pelletier, S. (1992) in *Analytical Ultracentrifugation in Biochemistry and Polymer Science* (Harding, S. E., Rowe, A. J., and Horton, J. C., eds) pp. 90–125, The Royal Society of Chemistry, Cambridge, UK
74. Malvern Instruments Limited (2014) *Microcal ITC200 System User Manual,* Malvern Instruments, Ltd., Worcestershire, UK
75. Tame, J. R., and Vallone, B. (2000) The structures of deoxy human haemoglobin and the mutant Hb Tyrα42His at 120 K. *Acta Crystallogr. D Biol. Crystallogr.* **56,** 805–811 CrossRef Medline
76. Fiser, A., and Sali, A. (2003) ModLoop: Automated modeling of loops in protein structures. *Bioinformatics* **19,** 2500–2501 CrossRef Medline
77. Jorgensen, W. L., Chandrasekhar, J., Madura, J. D., Impey, R. W., and Klein, M. L. (1983) Comparison of simple potential functions for simulating liquid water. *J. Chem. Phys.* **79,** 926–935 CrossRef
78. Berendsen, H. J., Postma, J. P., van Gunsteren, W. F., DiNola, A., and Haak, J. R. (1984) Molecular dynamics with coupling to an external bath. *J. Chem. Phys.* **81,** 3684–3690 CrossRef
79. Case, D. A., Cerutti, D. S., Cheatham, III, T. E., Darden, T. A., Duke, R. E., Giese, T. J., Gohlke, H.. Goetz, A. W., Greene, D., Homeyer, N., Izadi, S., Kovalenko, A., Lee, T. S., LeGrand, S., Li, P., Lin, C., *et al.* (2017) *AMBER 2017*, University of California, San Francisco
80. Shahrokh, K., Orendt, A., Yost, G. S., and Cheatham, T. E., 3rd. (2012) Quantum mechanically derived AMBER-compatible heme parameters for various states of the cytochrome P450 catalytic cycle. *J. Comput. Chem.* **33,** 119–133 CrossRef Medline
81. Frisch, M. J., Trucks, G. W., Schlegel, H. B., Scuseria, G. E., Robb, M. A., Cheeseman, J. R., Scalmani, G., Barone, V., Mennucci, B., Petersson, G. A., Nakatsuji, H., Caricato, M., Li, X., Hratchian, H. P., Izmaylov, A. F., *et al.* (2010) *Gaussian09 Revision D.01*, Gaussian Inc., Wallingford, CT
82. Wang, J., Wolf, R. M., Caldwell, J. W., Kollman, P. A., and Case, D. A. (2004) Development and testing of a general Amber force field. *J. Comput. Chem.* **25,** 1157–1174 CrossRef Medline
83. Humphrey, W., Dalke, A., and Schulten, K. (1996) VMD: Visual molecular dynamics. *J. Mol. Graph.* **14,** 33–38 CrossRef Medline
84. Michaud-Agrawal, N., Denning, E. J., Woolf, T. B., and Beckstein, O. (2011) MDAnalysis: A toolkit for the analysis of molecular dynamics simulations. *J. Comput. Chem.* **32,** 2319–2327 CrossRef Medline
85. Roe, D. R., and Cheatham, T. E., 3rd. (2013) PTRAJ and CPPTRAJ: Software for processing and analysis of molecular dynamics trajectory data. *J. Chem. Theory Comput.* **9,** 3084–3095 CrossRef Medline

Energetics underlying hemin extraction from human hemoglobin by *Staphylococcus aureus*

Megan Sjodt, Ramsay Macdonald, Joanna D. Marshall, Joseph Clayton, John S. Olson, Martin Phillips, David A. Gell, Jeff Wereszczynski and Robert T. Clubb

J. Biol. Chem. 2018, 293:6942-6957.
doi: 10.1074/jbc.RA117.000803 originally published online March 14, 2018